2018 25th Congress of International Federation for Heat Treatment and Surface Engineering

11-14 September 2018 | Xi`an China

PROCEEDINGS

Organized by Chinese Heat Treatment Society（CHTS）

25th IFHTSE CONGRESS PROCEEDINGS

11-14 September 2018

Xi'an China

Chinese Heat Treatment Society

Tel：+86（0）10 6292 0613 • Email：chts@chts.org.cn • Web:www.chts.org.cn

Add: 18 Xueqing Rd.,Beijing,China

Advanced Materials and Heat Treatment

Chemical-thermo Treatment

Effects of long-time thermal exposure on the microstructure and mechanical properties of CrMnFeCoNiAl0.25 high entropy alloy

Zhihong Zhong, Lijing Lin, Xin Xian, Yucheng Wu
(Hefei University of Technology)
zhong@hfut.edu.cn, ycwu@hfut.edu.cn

Abstract: Microstructure stability and its influence on the mechanical properties at elevated temperatures are important for the alloys used at high temperatures. The newly developed highentropy alloys have attracted for extensive interest for high temperature applications. In this work, the as-cast CrMnFeCoNiAl0.25 high entropy alloy was exposed at 700 ℃, to investigate the effects of long-time thermal exposure on the microstructure and mechanical properties. Samples were cut from the as-cast ingot and aged at 700 ℃ for 100, 1000, 2000 and 4000 h, respectively. The crystal structure of as-cast and aged alloys was analyzed by X-ray diffraction. Microstructure was obtained by a Sigma-Zeiss type scanning electron microscope and a transmission electron microscope, and micro-composition was analyzed by energy dispersive spectrometry. Mechanical properties were characterized in terms of compression and hardness tests, and samples after compression were prepared by ion milling for TEM observation to analyze the deformation behavior.

Results indicated that the as-cast CrMnFeCoNiAl0.25 alloy was not an equilibrium alloy to maintain single FCC structure at elevated temperature after aging. In the XRD patterns, some small diffraction peaks appeared around the angle of 43 °, with relatively low intensity, suggesting the formation of new phases. According to the SEM images, strip-like sigma phase and B2 phase were uniformly precipitated in the FCC matrix, confirmed to be Cr-rich phase and NiAl phase by EDS, respectively, and the phases subsequently coarsened when the exposure time increased. Owing to the effect of sluggish diffusion, elements could fully diffuse under high temperature and enough long-time. Cr element segregated and gathered together to form Cr-rich phase, while Ni and Al elements tended to form NiAl phase, due to their negative mixing enthalpy. Due to the increased volume fraction and the strengthening of hard precipitated phases, the yield strength and hardness increased greatly with increasing the thermal exposure time. The yield strength increased from 271.83 MPa for as-cast to 992.56 MPa for sample exposed for 2000 h. The hardness increased up to 322.35 HV for sample exposed for 2000 h. However, the yield strength decreased to 664.28 MPa after exposure for 4000 h, owing to the coarsening of precipitates. The alloy maintained good compressive ductility after aging.

Keywords: high-entropy alloys, aging, phase stability, mechanical properties

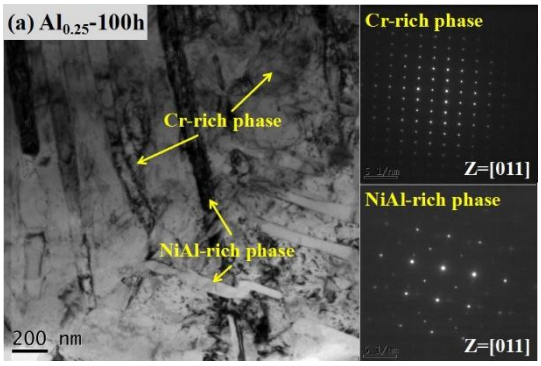

Fig.1

Influence of the quenching and partitioning process on the isothermal bainitic transformation kinetics in a lean medium manganese steel

Simone Kaar[1], Reinhold Schneider[1], Daniel Krizan[2], Christof Sommitsch[3]
(1. University of Applied Sciences Upper Austria;
2. Voestalpine Stahl GmbH; 3. Graz University of Technology)
simone.kaar@fh-wels.at

Abstract: Both, environmental and safety regulations force the automotive industry to the application of new steel grades combining both high strength and ductility. Recently, a high research effort has been put into the development of the 3rd generation advanced high strength steels (AHSS), including the concepts of quenching and partitioning (Q&P) and medium Mn steels. The Q&P process has been proposed as a promising approach for steel grades with a carbon-depleted martensitic matrix and retained austenitic islands. Typically, the microstructure of medium Mn steels consists of an ultrafine-grained ferritic matrix with approximately 30vol% of retained austenite. The medium Mn steels are characterized by an excellent combination of tensile strength and total elongation achieving the product of RmxA80 even more than 30 000 MPa·%.

The Q&P process of lean medium Mn steels is a novel approach for producing ultra-high strength and good formable steels with a mixture of martensitic-austenitic microstructure, where the meta-stable retained austenite undergoes the strain-induced martensitic transformation by the so-called transformation induced plasticity (TRIP) effect. In the present case, the retained austenite can be stabilized by C enrichment in the above-mentioned Q&P and medium Mn steels. Moreover, the presence of the hard-tempered martensitic matrix results in the superior performance of these steels in sheet cutting, bending and hole expansion operations. The majority of the models describing the Q&P process assume the full suppression of isothermal bainitic transformation (IBT) during the C partitioning process from martensite to austenite. However, the decomposition from austenite to carbide-free bainite during the C partitioning step has been observed in some instances. Therefore, the present work investigates the influence of the Q&P process on the transformation kinetics of the IBT in a 0.2C4.5Mn-1.3Al lean medium Mn steel.

Dilatometric experiments were carried out in order to evaluate the effect of the primary martensite formed during quenching on the IBT kinetics. Therefore, the Q&P annealing approach was compared to the TRIP bainitic ferrite (TBF) process, where the samples were directly quenched to the temperature of the IBT after the full austenitization. It was found that the formation of primary martensite in the Q&P samples led to an accelerated IBT. However, due to the presence of large amounts of primary martensite prior to the IBT, the Q&P samples contained a lower amount of bainite at the end of the IBT compared to the TBF ones. Furthermore, the transformation behavior was systematically studied with regard to the influence of the annealing parameters, such as the quenching temperature, the partitioning temperature and time. Especially at higher quenching temperatures, a pronounced influence of the partitioning temperature on the amount of bainite and its transformation kinetics could be observed. With increasing partitioning temperature, the amount of bainite formed decreased despite its accelerated transformation kinetics and therefore a larger amount of austenite could be retained in the final microstructure. With respect to the partitioning time, no significant influence on both, the amount of bainite and of retained austenite could be observed in the range from 150 s until 600 s.

The microstructure was investigated by means of light optical microscopy (LOM) and scanning electron microscopy (SEM). Using both methods, a martensitic-bainitic matrix with finely distributed retained austenite-islands was found. The amount of retained austenite was determined using the saturation magnetization measurement (SMM). Especially the quenching temperature had a significant impact on the amount of retained austenite, which varied between 5 vol% and 19vol%. Furthermore, the hardness according to Vickers revealed a further remarkable impact of the annealing parameters, such as quenching and partitioning temperature, on the predicted mechanical properties.

Keywords: quenching and partitioning, medium manganese, transformation kinetics, bainite

Enhance mechanical properties of sintered iron via surface grain size gradient

Yifei Chen, Guodong Cui
(School of Materials Science and Engineering, Southwest Jiaotong University)
gdcui@swjtu.edu.cn

Abstract: Porous material is an important part of materials science. But the porous material's strength is low, this paper uses high temperature to sinter the samples. Grain refinement was achieved by cycle quenching. The strength can be improved due to grain refinement strengthening. In this paper, Fe-N powder was used as raw material. The samples were prepared by sintering at high temperature in the high-temperature box furnace, then prepared ultrafine crystal iron alloy by cyclic induction quenching. The microstructures, grain size, mechanical properties of the samples were characterized by metallographic picture, Vickers hardness machine and universal testing machine. The experimental results attest that the sample who is carried out in the high temperature box furnace at 1100 ℃ for 30 min has the best mechanical property and the sample's density is 6.910 g/cm^3. We can observe from the metallographic picture the pores are uniform and small in all the samples. The samples under the premise of the above process, the optimal induction- heating time is 3S and the number of cycles is 6 times. The best process is decided by comparing the grain size, hardness and mechanical properties of the samples with different heating times and different cycles. This experiment has different quenching condition heating time and cycles are 0-0 times, 6S-2 times, 6S-6 times, 6S-10 times 6S-6 times, 5S-6 times, 4S-6 times, 3S-6 times. The samples used 0-0 times, 6S-2 times, 6S-6 times, 6S-10 times, there grain size is 16.67, 8.33, 6.67, 6.25 μm, there surface hardness is 120, 225.4, 269.4, 276 HV, there yield strength are 178, 292, 376, 425 MPa. The sample used 6S-6 times, 5S-6 times, 4S-6 times, 3S-6 times, there grain size is 6.67, 5.56, 4.17, 3.33 μm, there surface hardness is 269.4, 274, 285, 292.1 HV, there yield strength are 376, 467, 520, 615 MPa. The surface induction quenching process will not be harmful to the plasticity of the samples. At the same heating time, with the cycle times increase the grain size reduce. However, when cycle times greater than six, there grain size changes were not significant. Both surface and yield strength became harder and higher. At the same cycle times, with the heating time reduce the grain size reduce. Both surface and yield strength became harder and higher.

The grain size of the sample prepared by 3S-6 times can be refined to 3.33 μm, which is one-sixth than original samples. Surface hardness was 292.1 HV, which is double to that of original sample, indicating that grain refinement can enhance the hardness of the material. Compressed data show that the yield strength of the sample after 3S-6 times is 615 MPa, which is triple than the raw material. All in all, the sample with cyclic induction quenching not only improve the strength of material hardness, but also enhance the plasticity and material toughness. Grain refinement strengthening is an effective way to improve the samples' mechanical properties.

The best process of this experiment is decided that the samples carried out in the high temperature box furnace at 1100 ℃ for 30 min, the optimal induction heating time is 3S and the number of cycles is 6 times.

Keywords: bulk Fe-N alloy, grain size gradient, grain refinement strengthening, induction hardening

Microstructure, transformation and superelasticity characteristics of annealed Ti-Ni-Cr shape memory alloy

Zhirong He, Kangkai Liu, Hui Feng, Yuqing Du
(School of Materials Science and Engineering, Shaanxi University of Technology, Hanzhong, China)
hezhirong01@163.com

Abstract: The low-temperature superelasticity (SE) alloy can be widely used to make the accumulators, the vibrating controllers and the wear parts used in low-temperature environment, such as the polar research and the space probe, etc. At present, Ti-Ni based shape memory alloys that show SE above ambient temperature were fully investigated, while researches on low-temperature SE alloys were not studied yet. In order to develop a low-temperature SE alloy with superior properties, the Ti-50.8Ni-0.3Cr alloy was fabricated, and the effects of annealing processes on transformation, microstructure and SE of the alloy were investigated by means of differential scanning calorimetry, optical microcopy and tensile test. The following results are obtained:
1) The A→R/R→A type transformation occurs in Ti-50.8Ni-0.3Cr alloy annealed at 350-450 ℃, the A→R→M/M→R→A (A-parent phase B2, CsCl; R-R phase, rhombohedral; Mmartensite B19', monoclinic) type occurs in the alloy annealed at 500 ℃, the A→R→M/M→A type occurs in the alloy annealed at 550-600 ℃, and no transformation occurs in the alloy annealed at 650-800 ℃ upon cooling/heating. The influence of the tan on transformation behavior is not very. With increasing θ_{an}, the θ_R increases firstly and then decreases, the θ_M increases, and the $\Delta\theta_M$ decreases in the Ti-50.8Ni-0.3Cr alloy. The θ_R reaches maximum temperature 9.1 ℃ when anneals at 400 ℃. The θ_M reaches maximum temperature –80.2 ℃ when anneals at 600 ℃. The $\Delta\theta_M$ reaches maximum temperature 40.1 ℃ when anneals at 600 ℃. The $\Delta\theta_R$ changes in the range of 2.5-4.3 ℃. With increasing tan, the θ_R and θ_M increases firstly and then tends to constant, the $\Delta\theta_M$ decreases, and The $\Delta\theta_R$ changes in the range of 3.0-4.8 ℃. 2) When θ_{an}=350-500 ℃, Ti-50.8Ni-0.3Cr alloy is in the recovery stage, and the microstructure morphology is fibrous. When θ_{an}=550-600 ℃, the alloy is in the recrystallization stage, the microstructure is equiaxial, and the recrystallization temperature is about 590 ℃. When θ_{an}=600-800 ℃, the alloy is in the grain growth stage, and the microstructure is coarse grain. 3) The work hardening capacity and σ_b of Ti-50.8Ni-0.3Cr alloy annealed at 350-500 ℃ islarger than that of the alloy annealed at 550-700 ℃, while the δ_k of the latter is larger than that of the former. 4) With increasing θ_{an}, the critical stress of stress-induced martensitic transformation σ_M of the alloy decreases firstly and then increases, and the minimum value 311MPa is got at θ_{an}=450 ℃. The residual strain ε_R maintains at low level all the time when θ_{an}=350-600 ℃, and the ε_R increases sharply when θ_{an}>600 ℃. To obtain an excellent SE at room temperature for Ti-50.8Ni-0.3Cr alloy, the annealing temperature of the alloy should be lower than recrystllization temperature. 5) With increasing the numbers of stress-strain cycle, the SE of the alloy annealed at 350 ℃ and 600 ℃ changes gradually from partial nolinearity SE to complete nolinearity SE, while the one of the alloy annealed at 650 ℃ changes gradually from partial nolinearity SE to linear SE.

Keywords: Ti-Ni-Cr alloy, shape memory alloy, annealing treatment, transformation, superelasticity

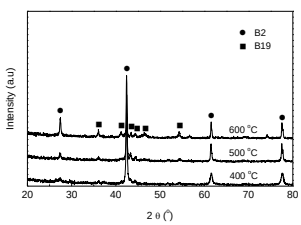

Fig.1

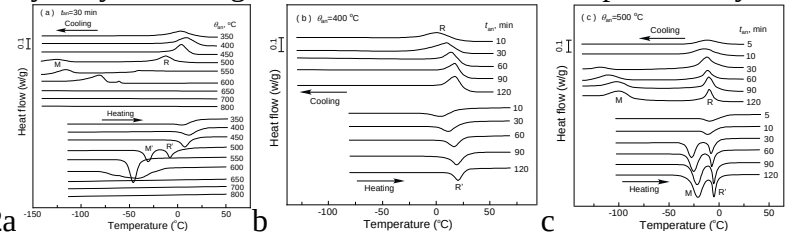

Fig.2a b c

Fig.1 XRD patterns of Ti-50.8Ni-0.3Cr alloy after annealing at different temperatures

Fig.2 Effect of annealing temperature θ_{an} (a) and annealing time tan at 400 ℃ (b) and 500 ℃ (c) on transformation behavior of Ti-50.8Ni-0.3Cr alloy

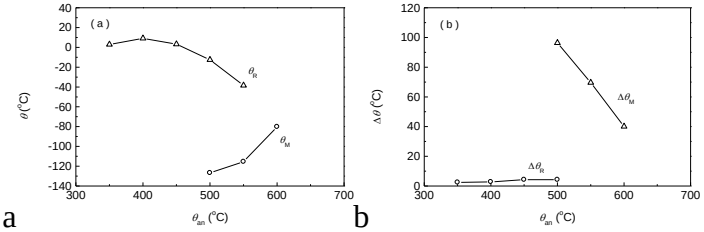

a b

Fig.3 Effects of annealing temperature on R and martensitic transformation temperatures (θ_R, θ_M) (a) and temperature hysteresises ($\Delta\theta_M$, $\Delta\theta_R$) (b) of Ti-50.8Ni-0.3Cr alloy after solution annealing at 800 ℃

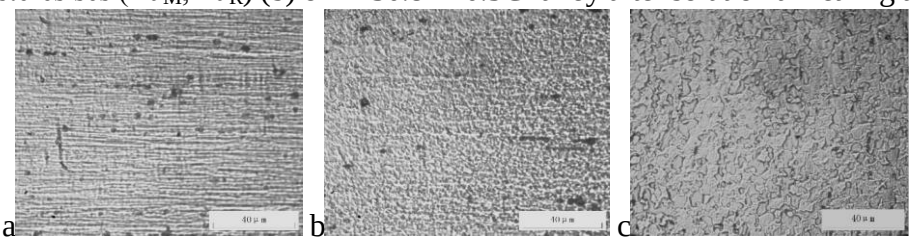

a b c

Fig.4 Microstructure of Ti-50.8Ni-0.3Cr alloy annealed at: (a) 570 ℃, (b) 590 ℃and (c) 600 ℃

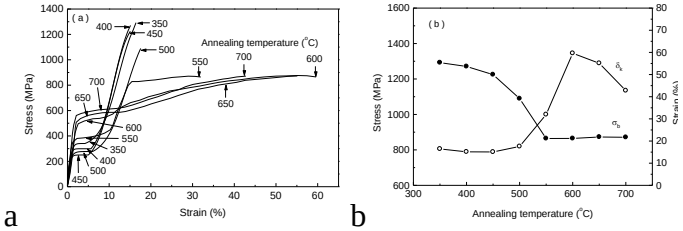

a b

Fig.5 Effect of annealing temperature on SE curves (a) and the critical stress of stress-induced martensite σ_M, the residual strain ε_R (b) of Ti-50.8Ni-0.3Cr alloy

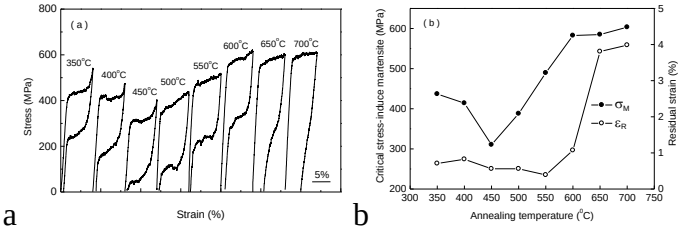

a b

Fig.6 Effect of annealing temperature on SE curves (a) and the critical stress of stress-induced martensite σ_M, the residual strain ε_R (b) of Ti-50.8Ni-0.3Cr alloy

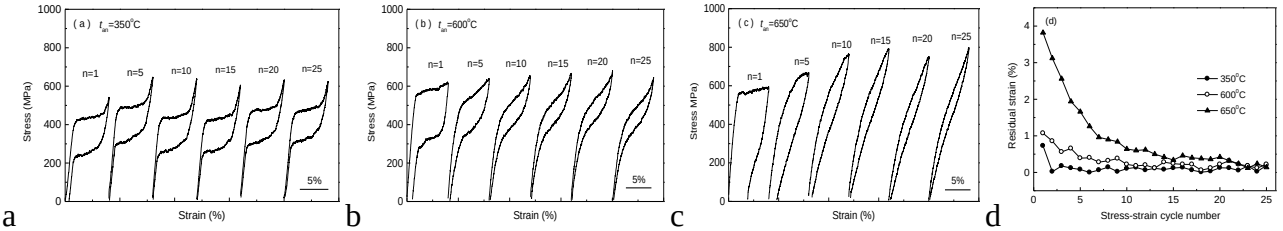

a b c d

Fig.7 Effect of stress-strain cycle on superelasticity curves (a), (b), (c) and residual strain (d) of Ti-50.8Ni-0.3Cr alloy annealed at 350 ℃, 600 ℃ and 650 ℃

Effect of annealing on transformation, microstructure and tensile properties of narrow hysteresis Ti-45Ni-5Cu-0.3Cr shape memory alloy

Yuqing Du, Zhirong He, Kangkai Liu, Hui Feng
(Shaanxi University of Technology)
hezhirong01@163.com

Abstract: In many SMAs, Ti-Ni based SMAs are of the best performance, not only good shape memory properties and superelastic properties, but also high strength, non-magnetic, corrosion resistance, wear resistance, good biocompatibility and high damping features. They have been applied in automotive, aerospace, construction, bridges, robotics, and biomedicine. Adding Cu in the Ti-Ni based alloys hardly changes the phase transition temperature and can reduce the phase transition temperature hysteresis and superelasticity stress, and a ternary Ti-Ni-Cu alloy with narrow temperature history and large shape memory strain was obtained. Moreover, the replacement of Ni in Ti-Ni alloy with Cu can reduce its cost. Adding Cr element in Ti-Ni based SMAs can reduce the phase transition temperature, improve the critical stress of stress-induced martensite and improve the mechanical properties of the alloy. In this study, the Ti-45Ni-5Cu-0.3Cr alloy was obtained by adding 5at% Cu and 0.3at% Cr in Ti-Ni alloy. The purpose of this paper is to study the effects of annealing temperature on transformation behavior, microstructure and tensile properties of Ti45Ni-5Cu-0.3Cr shape memory alloy were investigated by means of differential scanning calorimetry, optical microstructure and tensile tests. The results are as follows:

1) The A→M/M→A(A-parent phase B2, CsCl, M-martensite B19', monoclinic) type onestage transformation occurs in Ti-45Ni-5Cu-0.3Cr alloy annealed at 350-700 ℃ upon cooling/heating. The temperature hysteresis of the alloy is narrow (16.8-18.8 ℃), so the alloy is suitable for making fast response components.

2) The alloy annealed at 350-550 ℃ is in the recovery stage and the microstructure morphology is fibrous; the alloy annealed at 600-700 ℃ is in the grain growth stage and the microstructure morphology is equiaxed grains. The recrystallization temperature of the alloy is between 550-600 ℃.

3) With increasing annealing temperature, the martensite reoritation stress (σ_M), thetensile strength (σ_b) and the elongation of the alloy increase at first and then decrease. The σ_M and σ_b of the alloy annealed at 400-500 ℃ are excellent, and the plasticity of the alloy annealed at 650 ℃ is the best.

Keywords: Ti-45Ni-5Cu-0.3Cr alloy, shape memory alloy, annealing, transformation, tensile property

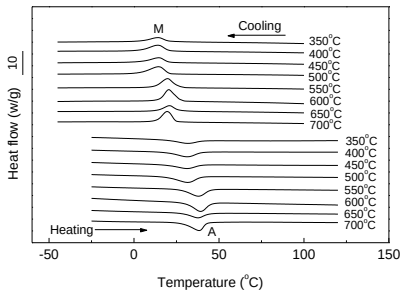

Fig.1

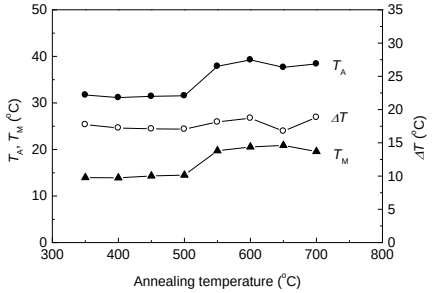

Fig.2

Fig.1 Effect of annealing temperatures on DSC carves of Ti-45Ni-5Cu-0.3Cr alloy

Fig.2 Effect of annealing temperature on A, M transformation temperature (TA, TM) and temperature hysteresis (ΔTM) of Ti-45Ni-5Cu-0.3Cr alloy

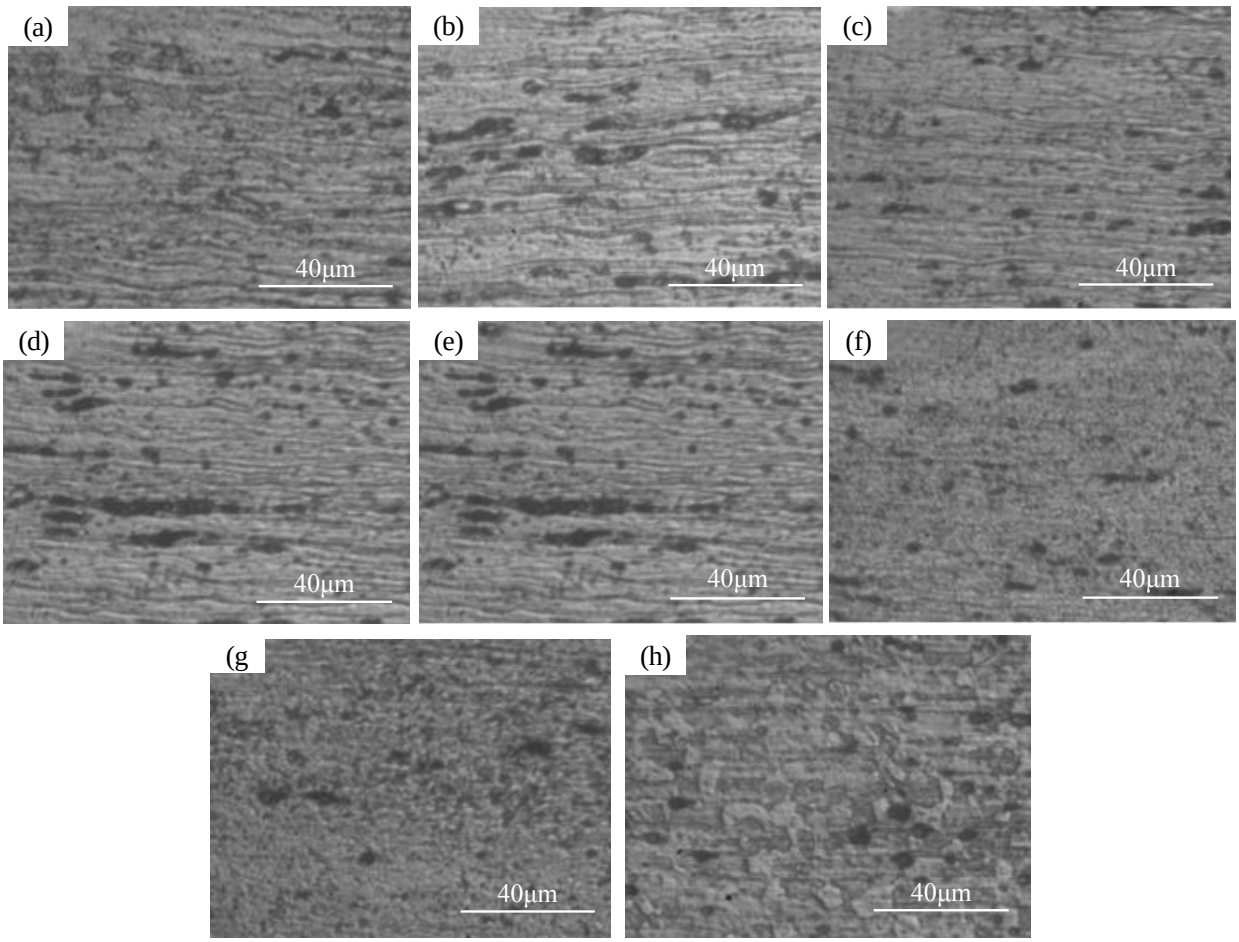

Fig.3 Effect of annealing temperature on microstructure of Ti-45Ni-5Cu-0.3Cr alloy: (a) 350 ℃; (b) 400 ℃; (c) 450 ℃; (d) 500 ℃; (e) 550 ℃; (f) 600 ℃; (g) 650 ℃; (h) 700 ℃

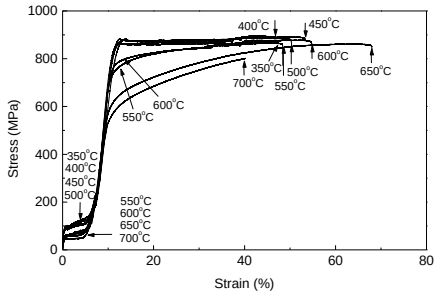

Fig.4 Effect of annealing temperature on stress-strain curves of Ti-45Ni-5Cu-0.3Cr alloy

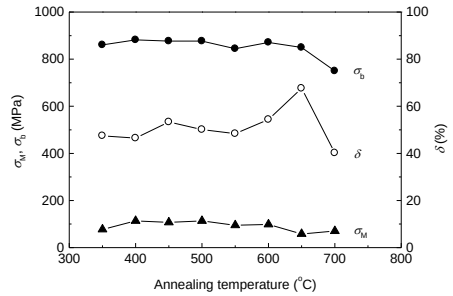

Fig.5 Effect of annealing temperature on martensite reorientation stress σ_M, tensile strength σ_b and elongation δ of Ti-45Ni-5Cu-0.3Cr alloy

Effect of annealing on transformation and shape memory effect of Ti-50.8Ni-0.1Nb shape memory alloy wire

Kangkai Liu, Zhirong He, Hui Feng, Yuqing Du
(School of Materials Science and Engineering, Shaanxi University of Technology, Hanzhong, China)
hezhirong01@163.com

Abstract: Shape memory alloys (SMAs) have been widely used in aerospace, machinery manufacturing, transportation, civil engineering, energy engineering, biomedicine, daily life and other fields because of their excellent shape memory effect (SME), superelasticity (SE), biocompatibility and high damping. At present, Ti-Ni binary shape memory alloys were fully investigated; while researches on Ti-Ni-Nb shape memory alloys were not fully. The purpose of this paper is to study the effect of annealing on the phase composition, phase transformation, microstructure and shape memory behavior of Ti-50.8Ni-0.1Nb alloy. The properties of the alloy were investigated by X-ray diffraction, differential scanning calorimetry, confocal laser scanning microscopy and universal tensile tester. The result is as follows:

1) Ti-50.8Ni-0.1Nb alloy was annealed at 350-700 ℃, the holding time was 30 min, furnace cooling. Within the annealing temperature (θ_{an}) range, the alloy consists of parent phase A (B2, CsCl) and martensite M (B19 ', monoclinic).

2) When 350 ℃≤θ_{an}≤450 ℃, the reversible transformation of A→R→M/M→R→A (R-R phase, rhombohedral) occurs, when 500 ℃≤θ_{an}≤550 ℃, the A→R→M/M→A occurs, and when 600 ℃≤ θ_{an} ≤ 700 ℃, the A→M/M→A occurs in Ti-50.8Ni-0.1Nb alloy upon cooling and heating. With increasing the θ_{an}, the positive and reverse R transformation temperatures (θ_R, θ_{Rr}) decrease, the positive and reverse martensitic transformation temperatures (θ_M, θ_{Mr}) increase firstly and then decrease, θ_M and θ_{Mr} reached the maximum of –34.71 ℃ and 26.11 ℃ respectively when annealed at 500 ℃. With the increase of θ_{an}, the R transformation temperature hysteresise $\Delta\theta_R$ change within the range of 6.7-9.8 ℃. the M transformation temperature hysteresise $\Delta\theta_M$ increases firstly and then decreases, $\Delta\theta_M$ reaches a maximum of 75.1 ℃ when θ_{an}=450 ℃.

3) With increasing the θan, the microstructure morphology of Ti-50.8Ni-0.1Nb shape memory alloy changes from fibrous to equiaxed grains, and the recrystallization temperature is about 580-600 ℃.

4) Ti-50.8Ni-0.1Nb alloy shows SME when 400 ℃≤θ_{an}≤550 ℃, and shows SE when θ_{an}=350 ℃ and θ_{an}≥600 ℃. The tensile strength of Ti-50.8Ni-0.1Nb alloy annealed at 350-550 ℃ is higher than that of the alloy annealed at 600-700 ℃, while the percentage elongation of the former is lower than that of the latter. The critical stress-inducing martensite (σ_M) decreases firstly and then increases, and the minimum value 311 MPa is got at θ_{an}=450 ℃.

5) The σ_M of Ti-50.8Ni-0.1Nb alloy reaches the minimum (256 MPa) and maximum (459 MPa) when θ_{an}=450 ℃ and 700 ℃, respectively. With increasing stress-strain cycling number, the σ_m of Ti-50.8Ni-0.1Nb alloy decreases. The stability of the SME in the alloy annealed at 400-550 ℃ and the SE in the alloy annealed at 600-700 ℃ is well.

Keywords: Ti-Ni-Nb alloy, shape memory alloy, transformation, microstructure, shape memory effect

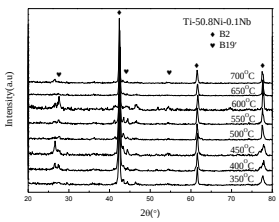

Fig.1

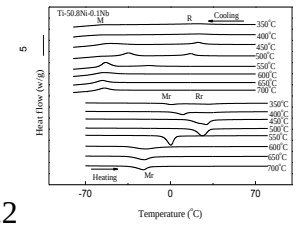

Fig.2

Fig.1 XRD patterns of Ti-50.8Ni-0.1Nb alloy wire annealed at 350-700 ℃

Fig.2 Effect of annealing temperature on phase transformation behavior of Ti-50.8Ni-0.1Nb alloy wire

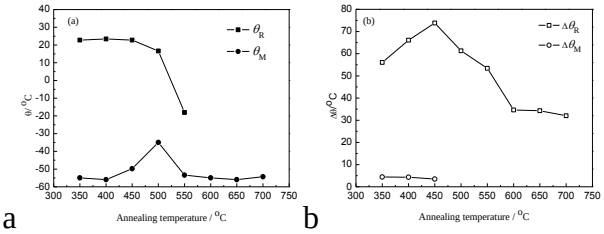

a b

Fig.3 Effect of annealing temperature on R and M transformation temperature(θ_R, θ_M)(a) and temperature hysteresises($\Delta\theta_R$, $\Delta\theta_M$)(b) of Ti-50.8Ni-0.1Nb alloy wire

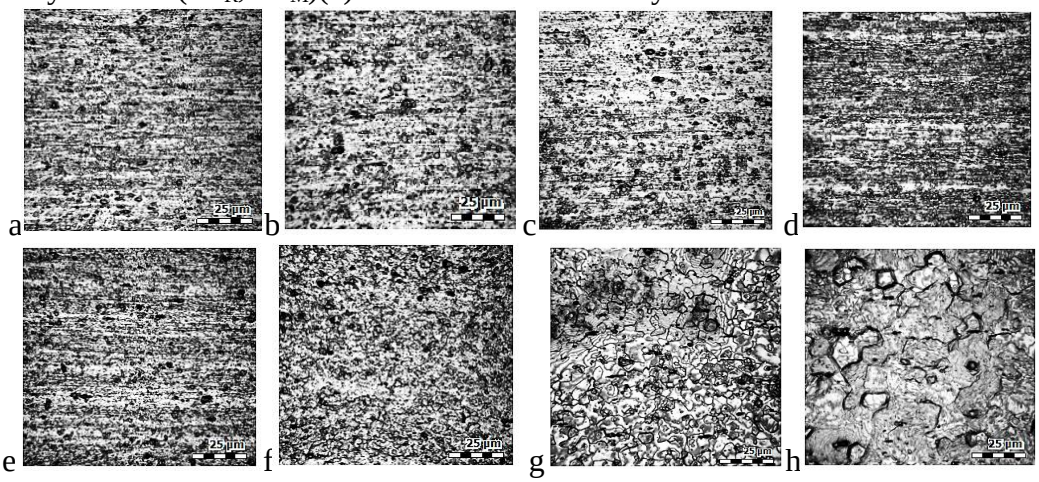

a b c d

e f g h

Fig.4 Microstructure of Ti-50.8Ni-0.1Nb alloy wire annealied at: (a)350 ℃, (b)400 ℃, (c)450 ℃, (d)500 ℃, (e)550 ℃, (f)600 ℃, (g)650 ℃and (h)700 ℃

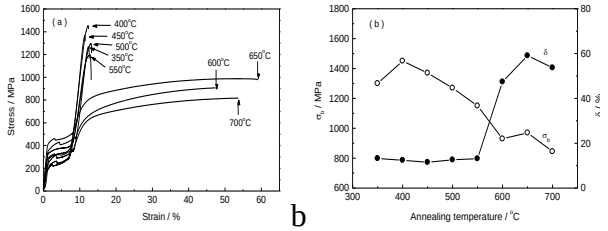

a b

Fig.5 Effect of annealing temperature on tensile curves (a) and tensile strength σb , percentage elongation δ (b) of Ti-50.8Ni-0.1Nb alloy

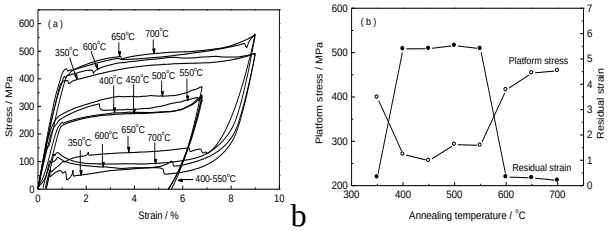

a b

Fig.6 Effect of annealing temperature on shape memory behavior (a) and platform stress, residual strain in stress-strain curves (b) of Ti-50.8Ni-0.1Nb alloy

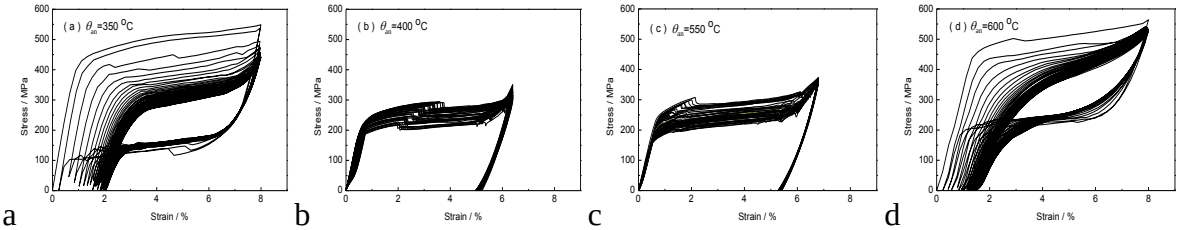

a b c d

Fig.7 Effect of stress-strain cycle on shape memory behavior of Ti-50.8 Ni-0.1Nb alloy annealed at: (a)350 ℃, (b)400 ℃, (c)550 ℃, (d)600 ℃

Effect of annealing on phase transformation and superelasticity of Ti-51.1Ni shape memory alloy

Hui Feng, Zhirong He, Kangkai Liu, Yuqing Du, Rongyao Ji
(School of Materials Science and Engineering, Shaanxi University of Technology, Hanzhong, China)
hezhirong01@163.com

Abstract: Ti-Ni based shape memory alloys (SMA) can be widely used because of their excellent shape memory effect, superelasticity, high damping property, biocompatibility, ray not permeability, high specific strength, nonmagnetic and wear-resisting performance etc. In order to develop an SMA with low-temperature superelasticity, the effects of the annealing temperature (Ta) on phase composition, phase transformation, microstructure and superelasticity in Ti-51.1Ni shape memory alloy were studied by means of X-ray diffractometer (XRD), differential scanning calorimetry (DSC), laser scanning confocal microscopy (LSCM) and tensile test in this paper. The results are as follows:

1) The composition phases of 350-700 ℃ annealed Ti-51.1Ni alloy, at room temperature, are martensite (M) (monoclinic structure B19′) and parent phase (A) (CsCl structure B2), and A phase is dominantly. The A→R→M/M→R→A type transformations occur in Ti-51.1Ni alloy annealed below 500 ℃ upon cooling/heating. The A→R→M/M→A type transformations occur in Ti-51.1Ni alloy annealed at 600 ℃ upon cooling/heating.

2) The A→M/M→A type transformations occur in Ti-51.1Ni alloy annealed at 650 ℃ upon cooling/heating. With the increase of Ta, the R transformation temperature TR and the reversal R transformation temperature TRr decrease, the M transformation temperature TM and the reversal M transformation temperature TMr increase firstly and then decrease, and TM temperature reaches to maximum 73 ℃ when T_a=600 ℃, T_{Mr} temperature reaches to maximum 13 ℃ when T_a=500 ℃. With increasing T_a, the temperature hysteresis ΔT_M of M transformation decreases, and ΔT_M decreases from 90 ℃ to 60 ℃ when increases from 500 ℃ to 600 ℃. The temperature hysteresis ΔT_R (about 4.5 ℃) of R transformation almost does not change with T_a.

3) With the increase of Ta, the microstructure morphology of Ti-51.1Ni shape memory alloy changes from fibrous to equiaxed grains, and the recrystallization temperature is about 600 ℃.

4) The strength of Ti-51.1Ni alloy annealed at 350-550 ℃ is significantly higher than that ofthe alloy annealed at 600-700 ℃, while the former's plasticity is less than the latter's.

5) Ti-51.1Ni alloy shows superelasticity at room temperature. With the increase of Ta, thecritical stress σ_M of stress induced martensite transformation decreases firstly and then increases, and the minimum 550 MPa can be gained when T_a=400 ℃. The superelasticity residual strain εr is very small (0.42%-0.48%) in Ti-51.1Ni alloy annealed at 350-550 ℃, and the ε_r is large (1.58%-1.67%) when Ti-51.1Ni alloy was annealed at 600-700 ℃. With the increase of the number of stress-strain cycles, the Ti-51.1Ni alloy annealed at 350-700 ℃ shows superelasticity constantly. To obtain the stable superelasticity, the alloy should be trained in stress-strain circulation.

Keywords: Ti-51.1Ni alloy, shape memory alloy, transformation, microstructure, superelasticity

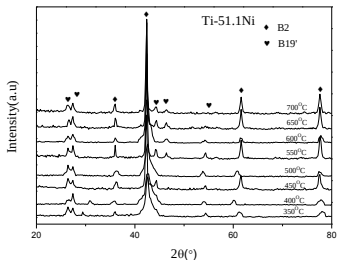

Fig.1 XRD patterns of Ti-51.1Ni alloy annealed at 350-700 ℃

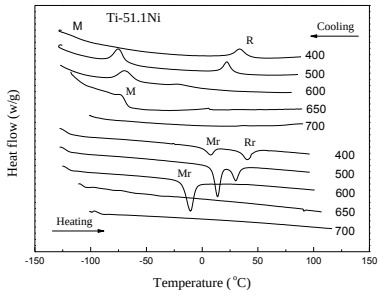

Fig.2 Effect of annealing temperature on phase transformation behavior of Ti-51.1Ni alloy

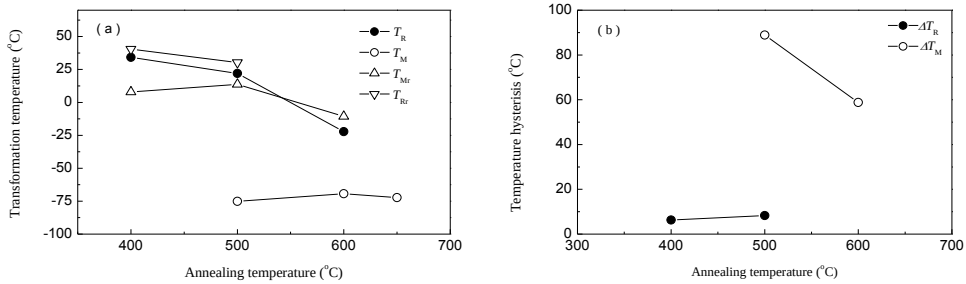

Fig.3 Effect of annealing temperature on transformation temperature: (a) and temperature hysteresis; (b) of Ti-51.1Ni alloy

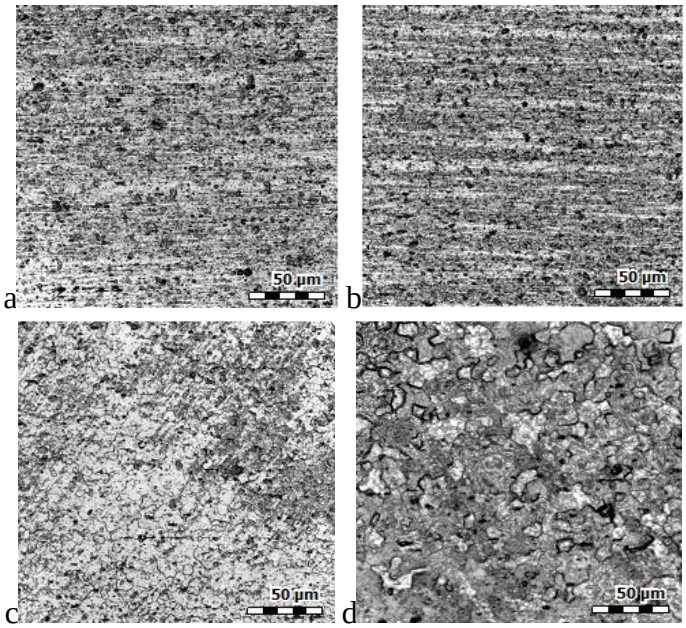

Fig.4 The microstructure of Ti-51.1Ni alloy wire annealed at: (a)400 ℃; (b) 550 ℃; (c) 650 ℃and (d) 700 ℃

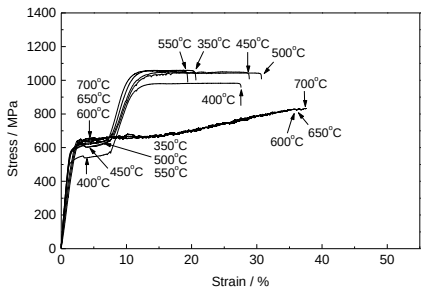

Fig.5 Effect of annealing temperature on tensile stress-strain curves of Ti-51.1Ni alloy

Characteristic of retained austenite decomposition during tempering and its effect on impact toughness in 2.25Cr-1Mo-0.25V steel

Zhonghua Jiang, Pei Wang, Xiangjun Chen, Dianzhong Li, Yiyi Li
(Shenyang National Laboratory for Materials Science, Institute of Metal Research, Chinese Academy of Sciences)
pwang@imr.ac.cn

Abstract: Granular bainite, which is composed of bainitic ferrite and blocky islands of retained austenite (RA) and/or martensite, is often obtained in 2.25Cr-1Mo-0.25V steel heavy forgings after quenching heat treatment. According to previous research, RA usually has a negative influence on the toughness properties of materials after high temperature tempering. In this study, the decomposition characteristic of RA at different tempering temperatures (TTs) of 2.25Cr-1Mo-0.25V steel is investigated, and then the decomposition products of RA are tentatively modified to improve the impact toughness by introducing a pretempering before 700 ℃ principal tempering.

The 2.25Cr-1Mo-0.25V steel blocks with dimensions of 65 mm×42 mm×42 mm were austenitized at 1050 ℃ for 2 h, and then air-cooled to ambient temperature. One group of samples were tempered at different temperatures of 180, 280, 350, 455 and 650 ℃ for 2 h only. The other group of samples were firstly pre-tempered at different temperatures of 180, 280, 350, 455, 550 and 650 ℃ for 2 h, and then subjected to a principal tempering at 700 ℃ for 4 h. Additionally, for the purpose of comparison, the principal tempering heat treatment is also carried out on the as-quenched sample directly, which is called as standard tempering in this manuscript. SEM, TEM and EBSD were used to analyze the microstructural evolution. Charpy impact tests at –18℃ were performed on a 450 J impact pendulum machine from Zwick. To analysis failure behavior of Charpy impact specimen, the fracture surfaces as well as cross-sectional areas beneath the fracture surface were observed by SEM.

The decomposition products of blocky RA islands show different variants at different TTs. When the TT is not higher than 350 ℃, the decomposition product mainly consists of martensite together with RA particles. The RA completely decomposes into fine bainite with high density of M_3C carbides at the TT of 455 ℃. When the TT further increases to 650 ℃, the decomposition product is composed of ferrite and Cr-enriched M_3C carbide particles, which are alternately arranged like a pearlite structure. While, the blocky RA decomposes into carbide clusters composed of $M_{23}C_6$ carbides and ferrite during standard tempering at 700 ℃. The microstructural observation of the broken impact samples reveal that those coarse $M_{23}C_6$ carbides formed along carbide cluster boundaries work to initiate the cracking or to facilitate the abrupt crack propagation into bainitic ferrites in a cleavage fracture mode, which results in the low average impact absorbed energy (60.7 J).

Accordingly, the size and distribution of $M_{23}C_6$ carbides within the carbide cluster can be modified by introducing a proper pre-tempering at the different temperatures ranging from 180 ℃ to 650 ℃ before principal tempering. The experimental results show that 455 ℃ is the optimal pre-tempering temperature to improve average impact absorbed energy of the steel (182 J). The microstructure observation reveals that during the 455 ℃ pretempering, the RA decomposes completely into bainite consisting of fine bainitic plates and high density of M3C carbides, which provide abundant nucleation sites for $M_{23}C_6$ carbides inside carbide clusters during subsequent 700 ℃ tempering, and thus avoid the formation of coarse $M_{23}C_6$ carbides along cluster boundaries.

Keywords: retained austenite, pre-tempering

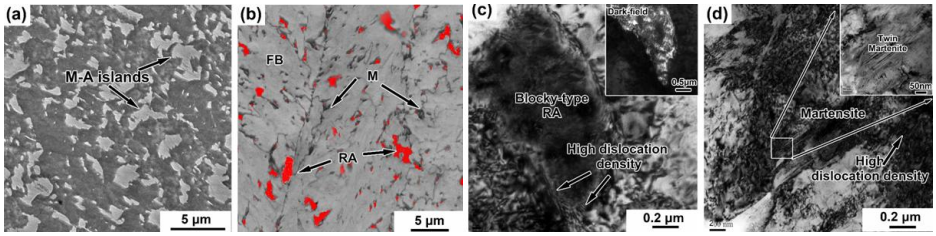

Fig.1 As-quenched microstructure of 2.25Cr-1Mo-0.25V steel: (a) SEM micrograph; (b) EBSD image quality map show different phases: BF: bainitic ferrite in grey, RA: retained austenite areas in red, M: martensite areas in in dark grey; (c) TEM micrograph show the blocky RA; (d) TEM show twin martensite

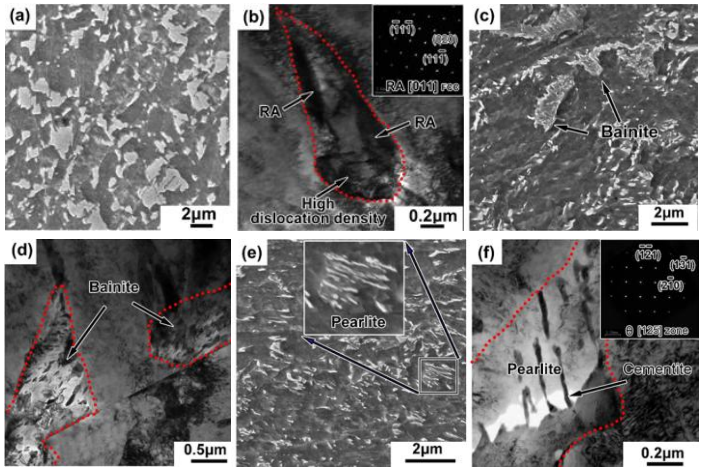

Fig.2 SEM and TEM micrographs showing the decomposition of RA at different: tempering temperatures: (a, b) 280 ℃; (c, d) 455 ℃; (e, f) 650 ℃, respectively

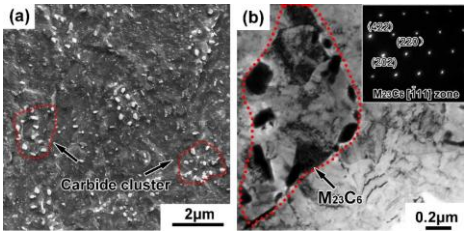

Fig.3 Microstructure showing the decomposition of RA in 700 ℃ standard tempered sample: (a) SEM micrograph, (b) TEM bright-field image

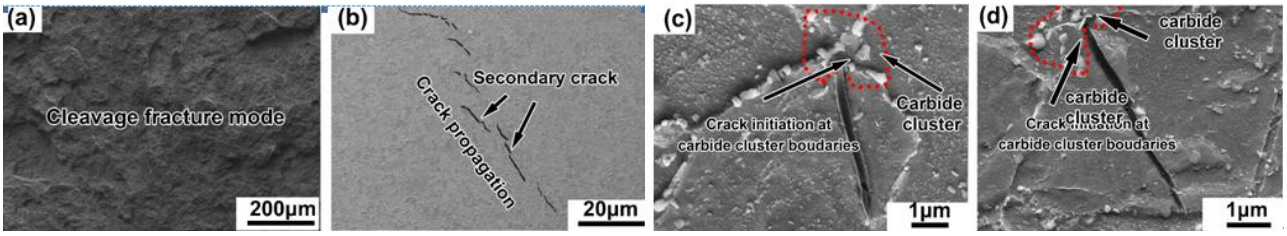

Fig.4 SEM micrographs showing (a) the fracture surface and (b, e) the cross-sectional area beneath the fracture surface of the standard tempering specimens

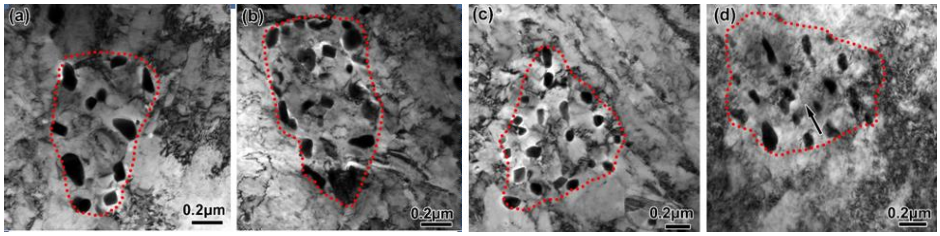

Fig.5 TEM micrographs showing carbide clusters in modified tempering treatment samples with different pre-tempering temperatures: (a) 180 ℃, (b) 350 ℃, (c) 455 ℃, (d) 650 ℃

Annealing of AISI 301 stainless steel before low temperature carburizing

Karl Andreas, Alexandra Friedrich
(Bodycote)
andreas.karl@bodycote.com

Abstract: One reason to choose austenitic stainless steels is the good formability. During cold working the strength can be increased significantly. AISI 301 as a metastable 17%Cr/7%Ni austenite is commonly used when elevated strength for thin walled components is required, especially for stainless spring applications. The alloy is non-magnetic when solution annealed but becomes magnetic when deformed to higher strength. Increased magnetism is mainly caused by α´-martensite formation.

As most austenitic stainless steels, albeit its good corrosion resistance, AISI 301 has a poor surface hardness leading to low abrasive/adhesive wear resistance and a tendency to galling.

To counteract these weaknesses, low temperature carburizing is chosen as a viable solution to enhance surface mechanical properties without altering the corrosion resistance. This thermo-chemical diffusion process forms carbon S-phase while avoiding carbide precipitation that would cause sensitization.

Mainly for high degrees of deformation it is possible that α´-martensite is a nucleation site for chrome rich precipitates. Dependent on number, type and distribution, it has been shown that these precipitates can deteriorate corrosion resistance. Several heat treatment options can reduce the α´-martensite content in a cold deformed stainless steel and reduce the probability of sensitization. The most common one, solution annealing, has the drawback that strength reduction of cold deformed grades is very high. Intermediate annealing between 500 and 700 ℃ has the capability to reduce the α´-martensite content without massively reducing base material strength. This annealing step can also increase the threshold for sensitization during low temperature surface hardening.

This paper shows the influence of pre-annealing of cold-deformed AISI 301 on the results of the surface hardening process, the base material properties and the resulting corrosion resistance of the material.

Samples with two degrees of deformation (ϕ=0.2, 0.6), one without deformation (ϕ=0) as reference were chosen. Four heat treatment states for each deformation were low temperature carburized and subsequently analyzed. Especially the highly cold-worked status (ϕ=0.6) showed a hardness reduction of 70% after solution annealing at 1050 ℃. Intermediate annealing at 600 ℃ reduced base material hardness by 13%. Annealing at 650 ℃ limited the reduction to 25% with a resulting base material hardness of 401 HV.

The latter processing route results in a favorable combination of properties with a base material hardness of 401 HV, comparable to UTS of 1300 MPa, very good surface hardness of 1100 HV0.05 and 13 µm diffusion depth as well as a pitting potential of 806 mV vs. NHE in 1% NaCl at 25 ℃.

Also, with regards to standard manufacturing technologies and other austenites, intermediate annealing prior to low temperature surface hardening has these advantages. During milling, turning or grinding, stresses are introduced on the surface which can cause α´martensite formation and –in combination with low temperature surface hardening- sensitization. Despite solution annealing or other high temperature heat treatments, the base material strength and parts geometry is nearly unaffected. This results in high strength compared with wear, galling and corrosion resistance.

Keywords: low temperature carburizing, stainless steel, cold-deformation

Effect of cryogenic treatment on microstructure and properties of D2 tool steel

Matteo Villa[1], Chloé Devos[2], Mikkel F. Hansen[3], Seunghwan Lee[3], Marcel AJ Somers[1]
(1. Technical University of Denmark, Department of Mechanical Engineering, Building 425, DK 2800 Kgs. Lyngby, DK;
2. Technical University of Denmark, Department of Mechanical Engineering, Building 425, DK 2800 Kgs. Lyngby, DK. Now with: Safran Aero Boosters, Route de Liers 121, 4041 Herstal, Belgium;
3. Technical University of Denmark, Department of Micro- and Nanotechnology, DTU Nanotech, Building 345B, DK-2800 Kgs. Lyngby, Denmark)
matv@mek.dtu.dk

Abstract: Intentional treatment of tool steels at cryogenic temperature has been reported to improve the mechanical properties, among which the resistance to wear. The mechanisms responsible for this improvement remain unexplained, despite various hypotheses. Literature data for D2 tool steel is extensive, wherefore this steel is the most promising candidate for additional investigation. In the present work, D2 steel was subjected to various austenitization treatments, followed by various cryogenic treatments and tempering treatments. The material's microstructure evolution and properties were investigated with synchrotron X-ray diffraction, scanning electron microscopy, vibrating sample magnetometry, hardness measurement and tribology tests. Data allows for a comparison to existing theories and to identify their shortcomings.

Austenitization treatments were performed at 990 ℃ for 30 or 60 min and at 1030 ℃ for 30 min. Cryogenic treatment consisted of: 1) immersion in boiling nitrogen followed by re-warming in water; 2) immersion in boiling nitrogen followed by storage in boiling nitrogen for 29 h or 72 h prior to re-warming in water; 3) cooling to boiling nitrogen temperature at a rate of 0.25 ℃/s followed by re-warming to room temperature at the same rate, interrupted by storage of the material 24 h at various temperatures in the range from –193 ℃ to –33 ℃. Tempering consisted of: (a) two cycles at 250 ℃ for 2 h; (b) two cycle at 600 ℃ for 2 h; (c) continuous heating to 677 ℃ at a rate of 0.1 ℃/s. In-situ Synchrotron X-Ray Diffraction analysis was applied to evaluate the evolution of the microstructure during tempering. Scanning electron microscopy was used to obtain information on the carbide populations and, more generally, on the microstructure of the material versus treatment conditions. In-situ magnetometry was applied to follow the austenite-to-martensite transformation as well as the evolution of magnetic hardness during cryogenic treatment. Finally, hardness and tribology tests were used to obtain an indication of the material's properties and performance for the treatment conditions.

Data showed that a certain fraction of retained austenite was always present in the material prior to tempering, independent of the austenitization conditions and cryogenic treatment applied. Cryogenic treatment reduced the fraction of retained austenite in the material. The austenite-to-martensite transformation during cryogenic treatment (BNT) was found to be partially a thermal, partially time dependent. A cryogenic cycle including prolonged storage at boiling nitrogen temperature reduced the fraction of retained austenite in the material, even though isothermal transformation at BTN was negligible. The isothermal martensite formation was accompanied by magnetic softening, which can be interpreted in terms of rejection of C from solid solution in martensite, supporting previous claims in the literature. Immersion in boiling nitrogen followed by immediate re-warming in water was sufficient to modify the response reaction of the material to tempering as well as its resistance to wear after tempering.

Keywords: cryogenic treatment, tool steel, synchrotron X-ray diffraction

Accelerating bainitic transformation by optimizing heat treatment

X. Y. Long, F. C. Zhang
(State Key Laboratory of Metastable Materials Science and Technology, Yanshan University, China)
lxy@stumail.ysu.edu.cn

Abstract: Carbide-free bainite, which exhibits high strength and plasticity, has been designed and manufactured in bearing, gear, railway (including rails and crossings) and other industries. Bainite transformation is controlled by the diffusion behavior of carbon at the bainite–austenite interface and by the drag effect of alloying elements, such as silicon, carbon, manganese, and chromium Bainite transformation in steels often requires a long isothermal transformation time. Consequently, the long isothermal transformation time and preparation period needed to obtain the bainite structure entail high economic costs and limit applications. Efficient control of the heat treatment process is the main method for rapid bainitic phase transformation. A medium-carbon bainitic steel has been designed, and the duration of the isothermal transformation in the tested steel at 300 ℃ is approximately 6521 s, and the proportion of incubation period (2024 s) is 31%. The phase composition and microstructure size of the tested steel are systematically optimized after a series of heat-treatment processes which are used to accelerate bainitic transformation, and the best heat treatment process for accelerating bainite transformation is obtained. In order to shorten the incubation period, ausforming process is used to shorten the incubation period. The entire process of bainite transformation can be accelerated by ausforming, while it is not suitable for actual production. After a 20 s transformation at 280 ℃ (Ms–10 ℃), incubation period at 300 ℃ isothermal transformation is significantly decreased, which is attributed to the preformed martensite provides more nucleation sites for bainitic nucleation. In order to shorten the transformation time, the two-stage isothermal transformation heat treatment process is designed. For two-stage isothermal transformation, one process is that samples are kept at 300 ℃ for 1200 s, then at 280 ℃ for enough time, and result shows that transformation time is significantly shorter than that of 300 ℃ isothermal transformation, which is attributed to increased nucleation driving force and secondary nucleation sites. The other process is that samples are kept at 315 ℃ (nose tip temperature) for 400 s, then at 300 ℃ for enough time, and result shows that incubation period and transformation time is significantly shorter than that of 300 ℃ isothermal transformation, which is attributed to the highest combined effect of transformation driving force and C atom diffusion rate. The size, distribution and volume fraction of the bainitic ferrite plates and retained austenite are also analyzed. The above heat treatment processes promote bainitic transformation and refine the microstructure. The study of a series of heat treatment processes provides a theoretical basis for actual production.

Keywords: bainitic transformation, heat treatment

A research on high-entropy alloys

Kefu Yao, Hengwei Luan, Zhidong Han
(Tsinghua University)
kfyao@tsinghua.edu.cn

Abstract: Recently, high entropy alloys (HEAs), a kind of multi-component alloys which consist of five or more elements in equal or near equal atomic ratio, have attracted lots of attentions of scientists and engineers due to that they usually possess simple crystalline structures and many excellent properties. Now the study of high-entropy alloys has become a frontier and hot research area within metallic alloys. It is known there mainly exist four kinds of effects in high-entropy alloys. They are high-entropy effects, sluggish diffusion effects, severe lattice distortion effects and cocktail effects. These effects would influence the microstructures and properties of high-entropy alloys. Here, the recent research progress of high-entropy alloys in Tsinghua university has been introduced. It shows that the NbMoTaWTi high-entropy alloys possesses high structure/property stability even after long term heat treatment at 1475 K. The Ti addition enhanced the both of the strength and ductility. It indicates Ti alloying is an effective way for improving the property of NbMoTaW alloy.

Keywords: high entropy alloy, mechanical property, microstructure

Microstructure and properties design in the laser cladded high-entropy alloy coatings through aging treatment

Yizhu He[1], Hui Zhang[1], Ye Pan[2]
(1. School of Materials Science and Engineering, Anhui University of Technology, Ma'anshan, China;
2. School of Materials Science and Engineering, Jiangsu Key Laboratory of Advanced Metallic Materials, Southeast University, Nanjing, China)
1223827114@qq.com

Abstract: Recently high-entropy alloys (HEAs) have attracted much interest in the materials community, as they offer massive opportunities to observe new phenomena, explore new structure and develop new materials with excellent mechanical properties, corrosion resistance and softening resistance at elevated temperature et al. Particularly, it is attractive to prepare high performance HEA coatings by laser-induced rapid solidification, which can be formed on the surface of components and parts in a variety of sizes and shapes with a lower cost in comparison with those bulk material fabrication methods. From the technical point of view, laser-induced rapid solidification could hamper the compositional segregation, improve the solubility in solid solution phases and lead to the strengthening effect by the grain refinement. The presentation report out recent work on typical microstructural features and mechanical and chemical properties in laser-induced rapidly solidified HEAs through component and aging treatment design, and compared them with conventional Co- and Ni- based alloy coatings. We also discuss some suggestions for future research and development in HEAs, from considerations of their characteristic properties.

Keywords: high-entropy alloys (HEAs), mechanical properties, coatings

Effect of Ti substitution for Al on the cuboidal nanoprecipitates in Al0.7NiCoFeCr2 high entropy alloy

Chunling Li, Qing Wang, Chuang Dong
(School of Materials Science and Engineering, Dalian University of Technology, Dalian 116024, China)
Wangq@dlut.edu.cn

Abstract: Coherent cuboidal B2 nanoprecipitation in body-centered-cubic (BCC) based high entropy alloys (HEAs) is important for the improvement of mechanical strength. The present work primarily investigated the effect of Ti substitution for Al on the cuboidal B2 nanoprecipitates in BCC Al0.7NiCoFeCr2 HEA. A series of (Al, Ti)0.7NiCoFeCr2 HEAs with different Al/Ti ratios were prepared by suction-cast processing, and their microstructures and mechanical properties were then characterized comprehensively. It was found that the substitution of Ti for Al can change the phase structures of ordered precipitation, from the B2-AlNi to a highly-ordered L21-Ni2AlTi phase. Especially, a small amount addition of Ti (≤4.2at%, Al/Ti ratio ≥2/1) renders the HEAs with cuboidal L21 nanoparticles coherently-precipitated into the BCC matrix, which is attributed to the moderate lattice misfit (0.5%-0.6%) between BCC and L21 phases. HEAs with such coherent microstructures exhibit high compressive yield strength of about 1700-1800 MPa. When the Ti content reaches up to 6.25at%, the matrix of the alloy will be turned into the (Fe, Co)Cr phase, rather than BCC, leading to a heavy brittleness.
Keywords: microstructure, phase transformation, strength, high entropy alloys, coherent precipitation

Flash lamp annealing of indium tin oxide thin-films deposited on polyimide backplanes

Seungho Park, Yoonsuk Kim
(Hongik University)
spark@hongik.ac.kr

Abstract: Xe-arc flashings of 0.4-1.0 ms in pulse duration annealed in diumtin oxide (ITO) thin-films deposited on flexible polymeric substrates at room temperature. As flexible substrates, highly transparent polyimide (PI) thin-films of 16 μm in thickness were prepared on a carrier glass. Measuring optical characteristics of the ITO and the PI thin films and using the Max well equations, we estimated complex refractive indices of ITO and PI materials. With the use of these optical properties, one dimensional conduction/radiation heat transfer simulation was carried out to predict the temperature variations in the specimens, assuring that the temperature in the ITO thin-film during the flash lamp annealing (FLA) process exceeded its crystallization point. Experimental FLA process resulted ina significant enhancement of the electrical conductivities as well as in a slight increase of optical transmittances of the specimen and was compared with the conventional furnace annealing (CFA) process of 1 h. Microscopic changes in the specimen during the annealing processes were compared using the X-ray diffraction pattern, atomic force microscope, and scanning electron microscope (SEM) measurements. Especially SEM images confirmed that sudden degradations in the electrical conductivities of ITO thin-films observed under higher power FLA or higher temperature CFA conditions were strongly related to the physical damages in the thin-films, which were incurred due to the thermal expansion mismatch between the ITO thin-film and the PI substrate at high temperatures.
Keywords: flash lamp annealing, indium tin oxide, polyimide substrate, flexible display, electrical resistivity

Control of thermal expansion in ZrW_2O_8-containing composites: effect of heat treatment

Qiang Zhang
(Harbin Institute of Technology)
zhang_tsiang@hit.edu.cn

Abstract: Zirconium tungstate, ZrW_2O_8, shows isotropic and negative thermal expansion properties from 0.3 K to its decomposition temperature of 1050 K. It is an ideal constituent of ultra-low thermal expansion composite materials used in electronics applications or high-precision optical instruments.
In this work, the ZrW_2O_8-containing aluminum matrix composites have been produced by a pressure infiltration technique. The large thermal mismatch stresses developed between the aluminum matrix and the ZrW_2O_8 particles during the fabrication cooling process led to the formation of the high-pressure gamma-ZrW_2O_8 phase. Subsequent heat treatment was used to reduce the content of gamma-ZrW_2O_8 in the composites, then the thermal expansion of the composites can be controlled in a desirable manner by adjusting the relative amount of gamma-ZrW_2O_8 and alpha-ZrW_2O_8. This research helps to understand the temperature-dependent expansion/contraction behavior of ZrW_2O_8-containing aluminum matrix composites.
Keywords: ZrW_2O_8, aluminum matrix composite, thermal expansion

Microstructure evolution, mechanical behaviors and ballistic performance of thelaminated composite of TiB_2-based ceramic and titanium alloy with nano-structured gradient

Zhongmin Zhao
(Department of Vehicle and Electric Engineering, Shijiazhuang School, Army Engineering University)

Abstract: Based on fusion bonding and atomic interdiffusion between the liquid ceramic and molten Ti-based alloy, the continuously-graded laminated composites of TiB_2-based ceramic and Ti-6Al-4V alloy were prepared by centrifugal thermal explosion processing. The laminated composites consist of 3-layer structure with the ceramic matrix, the intermediate and the Ti-based alloy substrate, and within the intermediate the continuous evolution of TiB_2, TiB and Ti-based phases in spatial size (i.e. microstructured→micro/nanostructured→nanostructured) developed. Interlaminar shear strength, flexural strength and fracture toughness of the composite measured 435±35 MPa, 1052±45 MPa and 65 ±15 MPa, respectively. FESEM fractographyies showed that because of the achievement of self-toughening mechanism by TiB_2 platelets and TiB rod-like grains along with limited ductile toughening mechanism by Ti-based phases in the composite, two kinds of load-displacement curves of interlaminar shearing test and 3-point bending test presented nearly the linear increase. By conducting DOP test with 14.5 mm army AP projectiles on TiB_2-based ceramic and the laminated composite, the average ballistic mass effectiveness of two materials measured 3.05 and 7.30. It was considered that because of the nano-structured gradient achieved from the ceramic to Ti-6Al-4V alloy, the acoustic impedance matching was improved between the ceramic and the alloy, while high bonding strength was maintained in the laminated composite, so the laminated composite not only presented high interlaminar cleavage resistance and high mechanical properties, but also exhibited high ballistic preformance by the dual mechanisms of interlaminar load transfer and multi-scale (micrometer-micro/nanometer-nanometer) interface shear-coupling.
Keywords: ceramic/metal laminated composite, centrifugal thermal explosion processing, nano-structured gradient, damage and failure, ballistic performance

Synthesis and crystallization kinetics of $Y_2CaAl_4SiO_{12}$ garnet-type glass-ceramic

Jiaxi Liu[1,2], Nan Lu[1,2], Gang He[1], Xiaoyu Li[3], Jianqiang Li[3], Jiangtao Li[1,2]
(1. Key Laboratory of Cryogenics, Technical Institute of Physics and Chemistry, Chinese Academy of Sciences, Beijing 100190, China; 2. University of Chinese Academy of Sciences, Beijing 100049, China; 3. Key Laboratory of Green Process and Engineering, Institute of Process Engineering, Chinese Academy of Sciences, Beijing 100190, China)
ipchg@mail.ipc.ac.cn

Abstract: $Y_2CaAl_4SiO_{12}$ garnet-type glass-ceramic was obtained by heat-treatment of the corresponding glass composition. The crystallization kinetics of the glass prepared by an aerodynamic levitation coupled with a laser heating system were investigated via differential scanning calorimetry (DSC). The effects of heat-treament temperature on the phase, microstructure, mechanical and optical properties of the prepared $Y_2CaAl_4SiO_{12}$ garnet-type glass-ceramic were studied. Crystallization of $Y_2CaAl_4SiO_{12}$ glass followed a two-dimensional growth mechanism with a calculated crystallization activation energy of 492.99 kJ/mol. The crystallized grains rapidly grown to a size over 100 nm with heat-treatment temperature increasing to 1000 ℃, which result in increased density (3.85 g/cm^3) and hardness (>10.05 GPa). The $Y_2CaAl_4SiO_{12}$ glass shows a high transmittance over 0.8 in the wavelength range of 650 to 4500 nm, and losses of transparency with increasing heat-treatment temperature.
Keywords: heat-treatment, garnet, crystallization, glass-ceramic

Study on transformation plasticity behavior of steels during austenite transformation

Shan Miao[1], Dongying Ju[1], Mengyuan Yan[1], Huijun Zhao[2]
(1. Saitama Institute of Technology; 2. Hangzhou Dianzi University)
dyju_mgcenter@163.com

Abstract: To predict the distortion of steels during heat treatment, the transformation plasticity behavior of the material was evaluated experimentally and theoretically. In this study, the influences of external tensile stress on transformation plasticity of 20MnCrS5 steels were experimentally investigated. The specimens were heated to 950 ℃ at a rate of 5 ℃/s, and the low external stresses of 0, 5, 10, 15 MPa were started to load just before the austenite transformation initiating temperature and completed after the austenite transformation. The results show that an increasing tensile stress introduced the decreasing distortion of the specimens during the austenite transformation. The strain of the transformation plasticity increases nonlinearly with the increase of stress and cannot be ignored. Based on the experimental results, a new mathematic model has been developed to describe the transformation plasticity behavior of steels during the austenite transformation. The model was implemented into the commercial FE code, COSMAP, via a user defined subroutine and the heat treatment process was modeled. Good agreements between the experimental and predicted data were obtained, which show that the determined model enables transformation plasticity during heat treatment process to be well predicted.
Keywords: transformation plasticity, austenite transformation, increase nonlinearly

Study on boiling phenomenon and thermal fluid behavior around circular plate during oil quenching process

Hideo Kanamori[1], Dongying Ju[1], Tsuyoshi Sugimoto[2]
(1. Saitama Institute of Technology; 2. Nissan Motor Co., Ltd.)
dyju_mgcenter@163.com

Abstract: When metal parts such as carbon steel and alloy steel are quenched with liquid medium that boiling point is lower than quenching temperature, high-temperature components will undergo intense boiling now they enter the medium. At the periphery of the metal parts, vapor particles are flocculated and a layer of evaporated film is formed. However, when the circular plate is quenched, the super-cooling of the upper surface and the lower surface of the circular plate is different, and the boiling instantaneous phenomena appearing at different positions are also different. The lower surface of the circular plate easily accumulates vapor particles, resulting in a thicker vapor-deposited film, resulting in non-uniform cooling of the circular plate. This phenomenon is one of the main reasons for the non-uniform deformation of metal parts during quenching. In this paper, the cooling curve of the lower surface of the circular plate in the first stage of nucleate boiling was measured, and the measured cooling curve truly reflected the behavior of the hot flow field during vapor particles formation in the first stage of nucleate boiling. In this paper, the high-speed camera is used to capture the thermal flow field during first stage of nucleate boiling and the formation of steamed air film in the nucleate boiling stage around the circular plate. The thermal fluid simulation of the first stage of nucleate boiling of the circular plate in the quenching of the oil medium is reproduced by the thermal fluid simulation of the mixed-phase flow model. It is explained that the effect of nucleate boiling and forming of the vapor film on temperature field and the strain field of the metal part after quenching.
Keywords: boiling, thermal fluid behavior, oil quenching

Identification of heat transfer rate by disk probe and validation of quenching simulation

Hideo Kanamori, Dongying Ju
(Saitama Institute of Technology)
dyju_mgcenter@163.com

Abstract: This paper proposes a method to determine the heat transfer coefficient of a SUS303 disk probe through the basic solution of the heat conduction equation. This method tests the cooling curve near the upper and lower surfaces of the disk, and substitutes the measured cooling curve into the heat conduction equation and determines the heat transfer coefficients of the upper and lower surfaces of the disk probe.

The results show that the heat transfer coefficient solved by this analytical method can not only reflect the transition from the first stage of nucleate boiling to film boiling, but also can clearly infer the difference in the heat transfer coefficient between the upper and lower surfaces of the disk probe. At the same time, this paper applies the same heat transfer coefficient to the simulation calculation of the quenching process, and improves the simulation accuracy of the quenching strain field.
Keywords: heat transfer rate, quenching, simulation

Issue in heat treatment of CSEF steels

Jeff Henry
(ATC-Engineering Services)
jzhou@atc-tn.com

Abstract: The heat treatment of the so-called Creep Strength Enhanced Ferritic (CSEF) steels – pressure part alloys such as Grade 91 – has been the source of many costly problems in the processing of these materials, largely because of a basic ignorance of the relatively complex metallurgy of these steels. These steels have been developed for one purpose: to provide improved long-term creep strength for pressure part applications in materials that have favorable thermos-physical properties, in particular thermal diffusivity and coefficient of thermal expansion. However, because of a poor understanding of the effects of the various heat treatments that are applied to these steels on their long-term creep strength, hundreds of millions of dollars have been spent in replacing mal-heat treated tubing, piping, valves and related pressure parts that were fabricated using these materials. A question that is frequently asked by both heat treaters and equipment operators is, "How many times can I heat treat a CSEF steel?" The question, itself, is utterly meaningless unless it is placed within the context of a specific heat of the steel and takes account of that heat's specific processing history. In this paper the various issues associated with the heat treatment of the CSEF steels will reviewed in detail and recommendations will be discussed of how Code rules can be revised to better control the effects of heat treatment – including multiple sub-critical heat treatments - in order to insure satisfactory material performance.

Keywords: heat treatment, CSEF steels

A new method of plasma strengthening in gun bore

Tianfang Luo
(Army Artillery Air Defense Academy)
luotianfang@qq.com

Abstract: Gun barrel is one of the most important parts of gun. In order to extend the service life of gun barrel and improve its anti-erosion and anti-wear performance, plasma quenching technique was succeed to treat the inner bore material. The microstructure and morphology of quenched hardened layer were analyzed with a metallographic microscope. The microhardness tester is used to measure the hardness of the surface and cross section of the hardened layer. Moreover, a friction and wear tester was performed to evaluate the friction and wear behavior of the plasma quenching. The results show that the gun barrel material is divided into three layers from the surface to the substrate after plasma quenching. The outermost layer is a martensitic hardened layer, and the deepest reaches 1.48 mm. Surface hardness increased from 320 HV to 725 HV and the maximum hardness is not at the surface but at the subsurface. Moreover, after plasma quenching, the average friction coefficient of the material was reduced by 30.2% and the surface abrasion resistance is improved by 11 times. The wear mechanism turned from adhesion wear to abrasive wear.

Keywords: erosion, plasma quenching

A hybrid thermal processing and coating method for enhancing the tribological properties of treated components

Johan BlomkVist[1], Fredrik Lindberg[2], Boris Zhmud[1]
(1. Applied Nano Surfaces; 2. Ovako A B)
johan.blomkvist@appliednanosurfaces.com

Abstract: Scoring, pitting and excessive wear are common lubricant-related failures which can be remedied by proper additive selection. Tribolayers formed on the tribologically loaded surfaces due to interaction with common EP/AW additives, such as ZDDP, MoS_2, sulfurized olefins or phosphate esters, are known to be very important for ensuring adequate surface integrity during component operation, especially in the boundary lubrication regime. Unfortunately, as performance requirements are being constantly pushed to the edge, this increases user dependency on specific lubricant types with very tight specifications. Various heat treatment methods – such as induction hardening, carburizing and nitriding are routinely used to improve component strength and longevity in demanding applications.
In the present communication, we present a new technology combining the well-known advantages of gas nitriding with a superior tribological performance profile of solid lubricant coatings. We call it the advanced thermal processing & coating (TP&C) technology, TriboNite®. Application of TriboNite® technology to special in-process strengthening hybrid steel allow us to achieve exceptional surface hardness upto 1200 HV – thus bridging the performance gap with traditional self-lubricated hard coating.
TriboNite® treated components exhibit higher resistance to bending and rolling fatigue which can be attributed to the existence of compressive stresses within the diffusion zone. They can withstand much higher shock loads and are much less sensitive to lubricant quality than reference stock components. Various solid lubricant layers – e.g. phosphate, borate, molybdenum disulfide, etc. - can be used to target specific applications requirements. Results of tribological, structural and surface-chemical studies of TriboNite®-treated component are also presented, with a special focus on gears.
material, machining and finishing methods, lubricant, and end-use are all important factors both for the early-life running-in behavior and life-long performance of tribologically stressed components such as gears, gear forks, chains, bearing rings, hydraulic pump housings and cylinder rods, ball studs, etc.
Keywords: thermal processing and coating, solid lubricant, nitriding processes, tribology, tribonite, coating

Enhanced mechanical properties of ultrahigh strength Mn-Si-Cr-C steels treated by a novel bainitic transformation plus quenching and partitioning process

Guhui Gao[1], Bingzhe Bai[2], Xiaolu Gui[2], Zhunli Tan[2], Yuqing Weng[2]
(1. Beijing Jiaotong University; 2. BJTU)
gaogh@bjtu.edu.cn

Abstract: In this paper, we attempt to review our recent works on the ultrahigh strength Mn-Si-Cr-C steels treated by BQ&P and BQ-P-T processes. The core of these novel processes is to incorporate the formation of carbide-free bainite during the initial quenching step (rather than partitioning step) of Q&P process and to achieve a fine multiphase microstructure (bainite + martensite + retained austenite). Our studies showed that the enhanced ductility, toughness and fatigue properties were achieved in the ultrahigh strength BQ&P and BQ-P-T steels, which is mainly attributed to the refined multiphase microstructures.
Keywords: bainite, quenching and partitioning, ductility, toughness

Study on aging heat treatment and stability control of aluminum alloy engine block

Ye Yan[1], Dongying Ju[2], Yuanqiang Tang[1], Daoqing Zang[1]
(1. SAIC General Motors Corporation Limited, China; 2. Saitama Institute of Technology)
dyju_mgcenter@163.com

Abstract: Face to China's fuel economy and CO_2 emissions regions improvement and environment friendly improvement in china's vehicle market, new generation engine was need fleet wide to satisfy fuel economy and CO_2 improvement. So that, SGM and GM jointed kicked off new generation engine studying, which called CSS.

Compare to benchmark in future global market, Audi 2.0L TFSI(EA888 Gen3 Pwt Class 2), BMW 2.0I L4 Twin Power (N20B20-OL) and Mercedes 2.0L L4. New generation engine need to touch these goals, high specific power, low RPM available transient torque, low BSFC, low NVH and less mass. Therefore a new product for increased stiffness and reduced weight cylinder block was designed, which was made from die casting plus T5 heat treatment process.

Here were some important technical items related material: 1) ultimate tensile strength, 2) yield strength, 3) high cycle fatigue strength (at 150 ℃), 4) elongation, 5) groth stabilization, 6) residual stress. Simple comparing on these items mentioned, the material property and mechanical performance was much high than last generation engine.

However, during design and process development of new generation cylinder block, there was aging stabilization of the aluminum alloy, which might lead to oil consuming unnormal or oil burned. Therefore, this paper would like deep dive this problem to find the root cause and take a series actions to meet technical items in this paper. Furthermore, some control methods into current heat treatment control standard, CQI-9 in the automotive will be discussed in this paper.

Keywords: aging heat treatment, stability control, aluminum alloy

Quench sensitivity of Al-7Si-0.2Mg high pressure vacuum die cast alloy

Mengyun Liu, Zhan Zhang, X. Grant Chen
(University of Quebec at Chicoutimi)
xgrant.chen@uqac.ca

Abstract: The quench sensitivity of Al-7Si-0.2Mg high pressure vacuum die castings was investigated by the time-temperature-transformation (TTT) and the time-temperature-property (TTP) curves with interrupted quench technique. The quench sensitive temperature range is from 250 ℃ to 450 ℃ and the nose temperature is around 350 ℃. The coefcients k2-k5, related to the nucleation kinetics of precipitates, of the TTP curves were determined. The mechanical property evolution as a function of quenching rates was predicted using the quench factor analysis method. It revealed that the quenching rate should be over 6 ℃/s to remain 95% of the maximum hardness. The precipitation of Mg_2Si phases in the castings was observed during isothermal treatment using a transmission electron microscope. Moreover, the quench sensitivity and kinetics of phase transformation of Al-7Si-0.2Mg alloy was compared to those of Al-10Si-0.5Mg alloys. It was found that the concentration of Mg and Si have significant influence on the quench sensitivity and phase transformation process of the high-pressure vacuum die castings.

Keywords: Al-Si-Mg alloy, high pressure vacuum die casting, quench sensitivity

Hot deformation induced evolution of the precipitations in an Al-Li alloy

Xiaoya Wang[1], Jiantang Jiang[1], Guo'ai Li[2], Liang Zhen[1]
(1. Harbin Institute of Technology; 2. Beijing Institute of Aeronautical Materials)
lzhen@hit.edu.cn

Abstract: Forming process as well as the resulted microstructure of highly alloyed Al-Cu-Li was highly sensitive to the condition of raw materials. The deformation behavior of an Al-Li alloy at homogenized and solution treated state was investigated using uniaxial hot compression (HC, 340-490 ℃, 0.001 to 1s^{-1}). The homogenized alloy presented obviously lower flow stress exhibiting better formability compared with the solution treated alloy when the HC temperature was below 420 ℃. The deformation activation energy of the homogenized alloy was 96.9 kJ/mol lower than that of the solution treated alloy, according to constitutive equations. Processing maps were generated to characterize the hot workability under various temperatures and strain rates. A mass of fine grains formed in the homogenized specimens while most secondary phases disappeared, indicating that recrystallization combined with dissolution occurred sufficiently during the hot compression process. The dominating deformation mechanism of the homogenized alloy was believed to be dynamic recrystallization. Elongated pancaked structure was observed in the solution treated and compressed specimen, indicating the occurrence of dynamic recovery. The particles stimulated nucleation (PSN) that related to coarse second phases in the homogenized alloy was believed to promote the recrystallization and alleviate the deformation instability. The current work suggested the possibility of obtaining improved workability and applicable recrystallized microstructure by tailoring the starting microstructure of the raw materials.

Keywords: Al-Li alloy, hot deformation, particles stimulated nucleation, workability

Improvement of fatigue strength of carburizing steel 20MnCrS5 during carburizing quenching

Shan Miao[1], Dongying Ju[1], Mengyuan Yan[1], Huijun Zhao[2]
(1. Saitama Institute of Technology; 2. Hangzhou Dianzi University)
dyju_mgcenter@163.com

Abstract: Carburizing quenching has a very important effect on metal fatigue strength. In this paper, carburizing steel 20MnCrS5 are heat treated respectively using existing condition and optimized condition. After carburizing quenching, the effects of different conditions on the hardness, microstructure and fatigue strength of carburizing steel are studied. Due to carburization, the near surface of the material will have the different microstructures with different carbon concentration. Select the surface layer, subsurface layer and heart tissue to prepare the fatigue samples and conduct fatigue test. By comparing the crack growth rate and fatigue limit to prove the correctness of the optimization conditions. The broke mouth shape of the impact fracture and broke mouth characteristic of the fatigue fracture of carburizing steel were observed and its influence regulation and mechanism of action on heat fatigue properties were also analyzed. The results show that the surface hardness of the samples are improved and fatigue performance at different depths are also improved.

Keywords: carburizing quenching, fatigue strength, hardness

Effects of solution and aging treatment on reverse austenite in 174PH stainless steel

Yixin Zhang[1,2], Yong Liu[1,3], Yudong Fu[2], Jingchuan Zhu[1,3], Zhonghong Lai[1,4]
(1. School of Material Science and Engineering, Harbin Institute of Technology, Harbin 150001, China;
2. College of Materials Science and Chemical Engineering, Harbin Engineering University, Harbin China;
3. National Key Laboratory for Precision Hot Processing of Metals,
Harbin Institute of Technology, Harbin 150001, China;
4. The Analysis and Testing Center of Harbin Institute of Technology, Harbin 150001, China)
1648862183@qq.com

Abstract: Precipitation hardened stainless steel 17-4PH has been widely used in the aerospace field, advanced turbines and steam turbine units, and the reactor structural materials in the domestic third-generation nuclear power plants. Reverse austenite is mainly present in martensite and precipitation hardened stainless steels. The presence and stability of the reverse austenite have a critical effect on the material properties. This paper intends to study the law of formation of inversion austenite in 17-4PH steel, analyze the influence of mechanism of process factors on the reverse austenite phase transformation, and reveal the mechanism of reverse austenite transformation of 17-4PH steel.

The effects of solution aging treatment on the reverse austenite in 17-4PH stainless steel were mainly studied in this paper by means of metallographic microscope, XRD, SEM and EBSD. The microstructure and the morphology, distribution and content of the reverse austenite in 17-4PH stainless steel under different heat treatment systems were observed.

First, the microstructure of the original sample was observed by metallography, SEM, and XRD, and it was found that it was mainly composed of ferrite, coarse low-carbon lath martensite, and some extremely fine second-phase particles. Afterwards, the other samples were heat treated in accordance with the following table 1.

After heat treatment of the samples, XRD, OM, SEM and EBSD were performed in order. At the same time combining XRD results with SEM and metallographic image analysis, it was shown that a single supersaturated Fe-Cr solid solution, namely lath martensite, formed in 17-4PH stainless steel during solution treatment. Pre-aged samples contained more martensite and the grains were refined very clearly. There were differently oriented martensite laths inside the grains, and fine carbides and other precipitate particles were dispersedly distributed between the martensite laths. After adding the final aging process, it was found that as the temperature increased, the austenite peak intensity gradually increased, but appeared abnormal at 590 ℃. When the temperature rised to 620 ℃, the austenite peak intensity was maximum, indicating that there was more reverse austenite formation at this time.

According to the EBSD image and the austenite phase boundary map (Figure 1), it was found that more precipitates appeared on the substrate after the final aging treatment was added. As a whole, the precipitates increased with the increase of temperature, and the crystal grains became finer. Especially after aging at 620 ℃, the content of precipitates on the substrate was the highest, and the grains are almost all small particles. In Fig.1, red indicates austenite, and in combination with its distribution and austenite content in Table 2, there was a large amount of retained austenite distributed on the substrate in the original sample, which was irregular in shape and large in size. As the aging temperature increaseed, the content of the reverse austenite gradually increased and increased abruptly at 560 ℃, and reached the maximum at 620 ℃. In addition to being distributed on the grain boundaries, the reverse austenite was also largely distributed on the martensite lath. However, at 590 ℃, the amount of reverse austenite is slightly less, which was consistent with the results of XRD analysis. The results showed that the content

of austenite was not only increased with the increase of temperature, but also changed in the special temperature range.

Through the above test and analysis of results, it was found that the reverse austenite was formed at the final stage of aging treatment and was mainly located at the grain boundary and between the martensite laths. The phase content at 620 ℃ was up to 19.02%, but the reverse austenite content was not only increases with increasing temperature, there was a special temperature range to promote its transformation.

Keywords: 17-4PH stainless steel, heat treatment, reverse austenite

Table 1 Heat treatment process at different temperatures of 17-4PH stainless steel

No.	Solid solution	Pre-aging	Final aging
1	1038 ℃,1 h, Air-cooled	—	—
2			—
3		816 ℃, 0.5 h, Air-cooled	500 ℃,3 h, Air-cooled
4			530 ℃,3 h, Air-cooled
5			560 ℃,3 h, Air-cooled
6			590 ℃,3 h, Air-cooled
7			620 ℃,3 h, Air-cooled

Table 2 Austenite content at different heat treatment conditions

No.	a	b	c	d	e	f	g	h
Phase content/%	12.71	0.11	0.13	0.87	1.31	8.17	5.56	19.02
Remarks		retained austenite				reverse austenite		

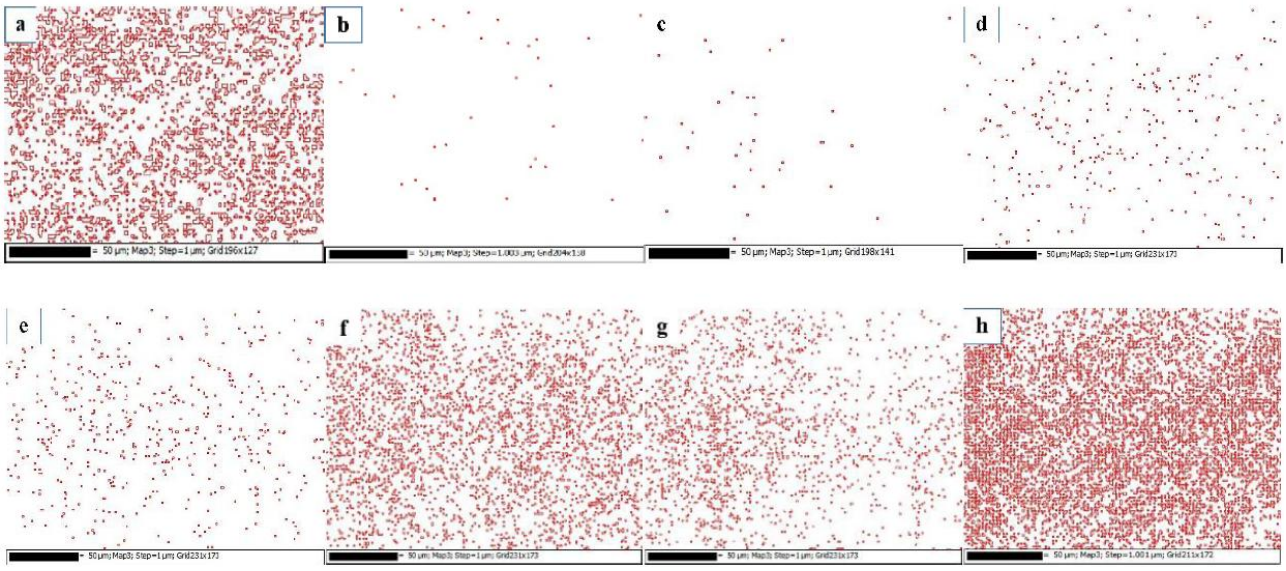

Fig.1 17-4PH stainless steel austenitic phase boundary map: (a) original sample; (b) solution treatment; (c) solution treatment+pre-aging treatment; (d) final aged at 500 ℃; (e) final aged at 530 ℃; (f) final aged at 560 ℃; (g) final aged at 590 ℃; (h) final aged 620 ℃

Phase transition of two-dimensional oxide crystal from topological phase to perovskite

Fei Zhou[1,2], Zhonghong Lai[4], Yong Liu[1,3], Jingchuan Zhu[1,3]
(1. School of Materials Science and Engineering, Harbin Institute of Technology, Harbin 150001, China;
2. MIIT Key Laboratory of Critical Materials Technology for New Energy Conversion and Storage, School of Chemistry and Chemical Engineering, Harbin Institute of Technology, Harbin150001, China;
3. National Key Laboratory for Precision Hot Processing of Metals, Harbin Institute of Technology, Harbin150001, China;
4. Analysis and Testing Center, Harbin Institute of Technology, Harbin 150001, China)
fgms@hit.edu.cn

Abstract: Perovskite oxides, as one kind of typical dielectric and ferroelectric material, have been widely studied due to their important applications in sensors, actuators, and information storage devices. However, there are scarce reports on their two dimensional (2D) counterpart, because there remains a bigger challenge in fabricating free-standing 2D perovskite oxides. Here, a novel research method initiated by theoretical calculations and design of a 2D growth model of hydrate precursor and followed by experimental fabrication and heat treatment aimed to phase transition to perovskite, was developed.

Density functional theory was used to design the 2D growth model. Layered potassium niobates 3D crystal structure was built with the atomic ratio of K:Nb=1:1. Fig.1(a),(b),(c) show fully relaxed precursor crystal model which have strong energy anisotropy between x-y plane and z direction, as shown in Fig.1(d), indicating a (001) facet preferable 2D growth.

Improved hydrothermal method was developed to synthesize 2D hydrate precursor. Hexagonal sheets with multiple size were obtained, see inset SEM image. The structure characterization show the in-plane structural information of as grown hydrate sheet (red line in Fig.2). Their main peaks are in accordance with the simulated spectrum (blue line in Fig.2) by DFT model. The experimental results verified the validity of theoretical prediction.

After annealing, the orthorhombic perovskite phase was obtained. The direct evidence for the phase transition from hydrate to perovskite phase is revealed in the difference in Raman shifts of the 2D sheets before and after annealing. The Raman shift of as-grown sheets before annealing is dominated by high frequency A1g modes (Fig.3a), which arises from the in-phase stretching of terminal Nb-O short bonds, indicating the lack of Nb-O-Nb bridge connection of each octahedrons in the hydrate phase. As compared with the hydrate case, multiple Raman peaks showed up (Fig.3b), especially the band around 550 cm^{-1} to 650 cm^{-1}, which signifies the linkage of oxygen octahedrons via the bridging oxygen atoms. Fig.3c shows the Raman shift of a sample with a thickness of 200 nm. Several surface modes, such as peripheral Nb-O A1g stretch modes (around 884 cm^{-1}) and T2g bending modes (around 400 cm^{-1}) are obtained in this spectrum. The 1.5 μm thick sample (Fig.3c)shows Raman shifts characteristic of bulk $KNbO_3$. which demonstrates that above-mentioned surface modes will be obscured as the bulk modes become more significant with increasing thicknesses. Valence change form Nb4+(hydrate) to Nb5+(perovskite) also give rise to the solid evidence for such a phase transition, as shown in the XPS analysis in Fig.3 f, g.

Our results demonstrate that perovskite niobates can be synthesized as 2D materials with multiple size. Three steps, including theoretical calculation and model design, hydrate sheet growth, and high temperature annealing, are used to obtain the final perovskite phase. This novel material synthesis method can be adapted for other material system, which potentially opens new opportunities for synthesis using traditional hydrothermal methods.

Keywords: 2D perovskite, phase transition

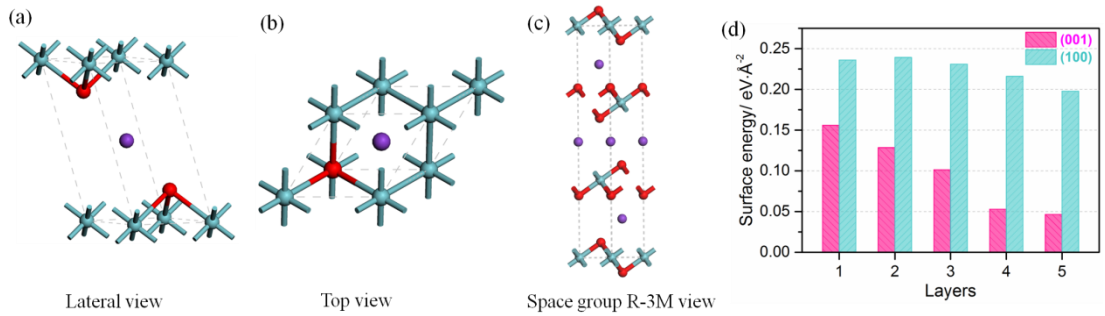

Fig.1 (a-c) as built molecular structure of $K(NbO_2)$ model: (a) lateral view, (b) top view, (c) the view of space group of R-3M; (d) DFT calculation results of $K(NbO_2)$ for preferable growth facets of (001) and (100)

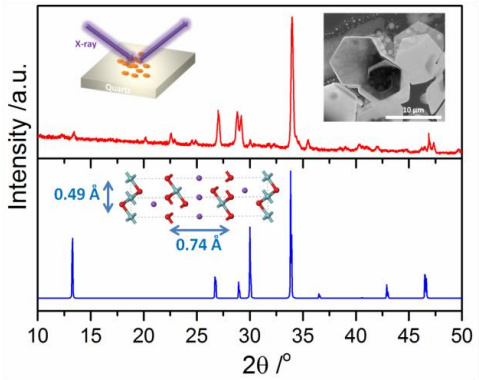

Fig.2 XRD results of as grown thin sheets (red), simulated XRD of calculation model after modification with extended x, y, z lattice parameter

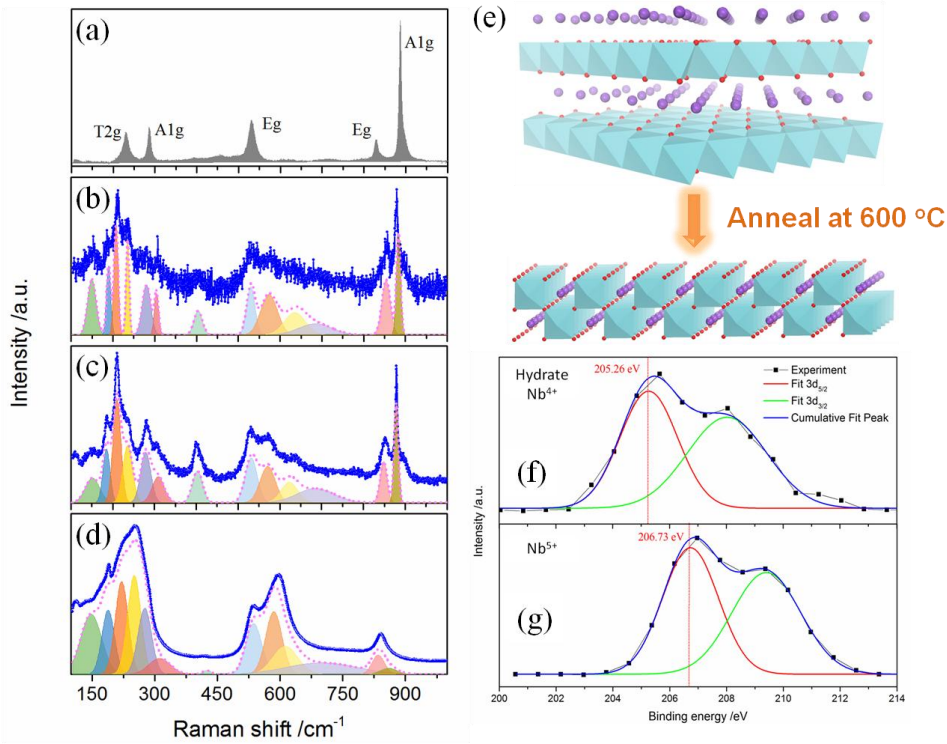

Fig.3 Raman spectra analysis: (a) as grown hydrate sample; (b) sample of 60 nm after annealing: (c) sample of 200 nm after annealing; (d) sample of 1.5 μm after annealing; (e) phases transition sketchmap; XPS spectra of Nb in samples: (f) as grown hydrate sheet; (g) $KNbO_3$ sample

Parameters optimization design of quenching and partitioning based on artificial neural network and particle swarm optimization

Mingqing Liao, Zhonghong Lai, Lujin Min, Yong Liu, Jingchuan Zhu
(Harbin Institute of Technology)
fgms@hit.edu.cn

Abstract: The matching among strength and toughness in high-strength steels has been always given the most attention by researchers in iron and steel industry. Recently, a novel heat treatment named "quenching and partitioning" (Q&P) has been proposed, such treatment provides a good way to improve the toughness of high-strength steel by stabilizing retained austenite. However, there are more than two parameters in Q&P. As a result, for a new material, it remains challenging how to get the best parameters in low cost way. Here a novel workflow, which combines orthogonal experimental design (OED) with artificial neural network(ANN) and particle swarm optimization(PSO), is adopted to explore the relationship between quenching and partitioning process parameters and properties in Fe 0.65wt%C-1.50wt%Si-0.91wt%Mn-1.08wt%W steel.

The austenitizing process was designed as tempering at 860 ℃ for 15 min. The quenching temperature (QT) range from 140 ℃ to 200 ℃, and 5 min to 20 min for partitioning temperature(PT) and 300 ℃ to 400 ℃ for partitioning time (Pt). The mechanical properties was implemented according to GB/T 228.1-2010 on Istron-5569 universal tensile testing machine with strain rate of 2 mm/min. The schematic representation of the optimization procedure is shown as Fig.1. OED provides experimental data for ANN model, including the inputs (here is QT, PT and Pt) and outputs (here means total elongation (Elt), reduction of area (RA), yield strength (YS) and ultimate tensile strength (UTS)). After training, the ANN model will be used to predict mechanical properties by inputting heat-treatment parameters. When combined with some optimization algorithm (here is PSO), the trained ANN model can be used to optimize heat-treatment parameters by properties. In this paper, L16(43) orthogonal array was used to design orthogonal experiment. To guarantee the capability of generalization, the Bayesian regulation was used as training algorithm. Before training, the input and output value was normalized to [0.1, 0.9]. The data got by orthogonal experiments were all used for training, and four additional experiments were implemented for validation.

This method provides a solution for parameters optimization of Q&P heat treatment in a cost-conserving way. The relationship between Q&P parameters and mechanical properties is established by ANN model. Compared with traditional heat treatment, the elongation of 167-367-5.0 (best parameters in Elt) increases by 146% times with no loss in YS and a little improvement in UTS.

Keywords: parameters optimization, quenching and partitioning, artificial neural network, particle swarm optimization

Table 1 The processes and corresponding mechanical properties optimized by PSO. Objective function is the target that need to be optimized, and constrain means all of the four properties are greater than those handled by traditional process

Objective function	Without constrain					With constrain				
	Parameters	El_t/%	*RA*/%	*YS*/MPa	*UTS*/MPa	Parameters	El_t/%	*RA*/%	*YS*/MPa	*UTS*/MPa
El_t	200-400-5.3	22.5	39.9	1316	1672	167-367-5.0	18.7	50.1	1707	1817
RA	140-374-5.0	17.1	52.0	1824	1864	145-375-5.0	17.3	52.0	1815	1855
YS	140-378-7.4	16.8	51.8	1826	1866	140-378-7.4	16.8	51.8	1826	1866
UTS	180-300-5.0	15.7	30.5	1279	2290	145-313-11.1	9.6	35.8	1714	2073
$UTS \cdot El_t$	200-300-15.5	19.6	41.7	1380	1982	167-367-5.0	18.7	50.1	1707	1817
Q&T		7.6	35.8	1707	1814	-	-	-	-	-

Note: Traditional process (Q&T) is heating to 860 °C followed by quenching to room temperature, then carrying out a tempering at 420 °C for 1 hour.

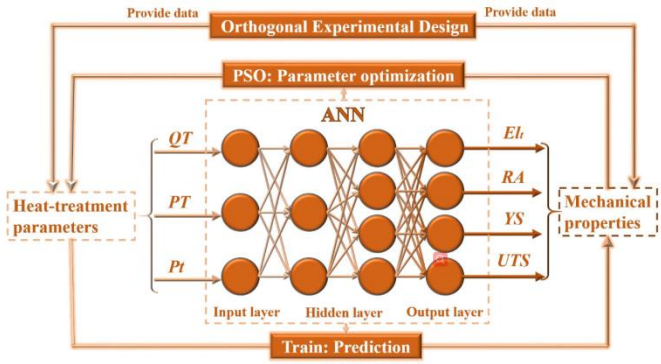

Fig.1 Schematic representation of the comprehensive method used in this work

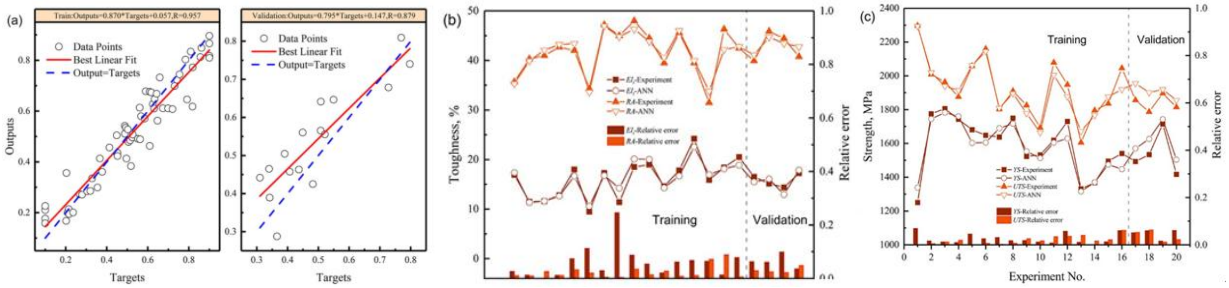

Fig.2 The training and validation of ANN model in this study: (a) The training and validation for ANN; The predicted and experimental (b) Elt, RA (c) YS, UTS and relative error

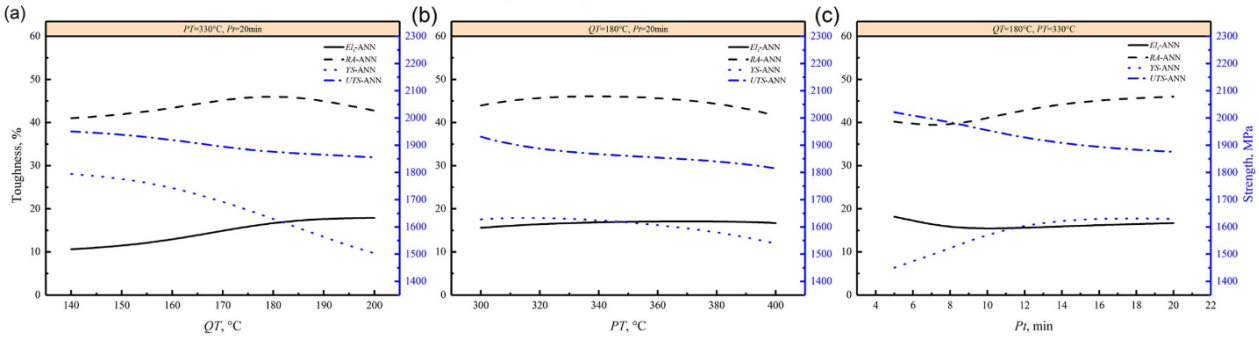

Fig.3 The effect of single heat treatment parameter: (a) QT; (b) PT; (c) Pt on mechanical properties parameters optimization

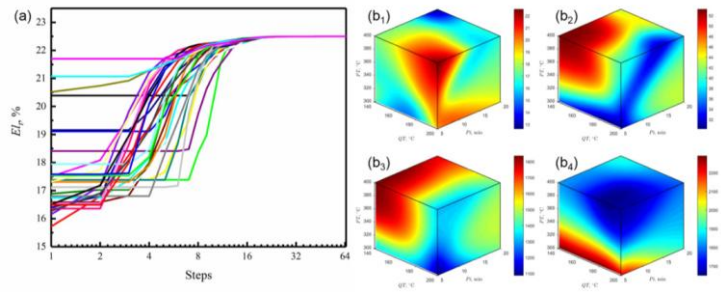

Fig.4 (a) the PSO's searching procedure of elongation without constrains and corresponding mechanical properties (b1) Elt; (b2) RA; (b3) YS; (b4) UTS around the optimal parameters

Effect of two-step Q&P treatment on microstructure and mechanical properties of 65Si2MnWA steel

Aorigele Bao[1], Mingqing Liao[1], Zhonghong Lai[1,3], Yong Liu1[2], Jingchuan Zhu[1,2]
(1. School of Material Science and Engineering, Harbin Institute of Technology, Harbin 150001, China;
2. National Key Laboratory for Precision Hot Processing of Metals, Harbin Institute of Technology, Harbin 150001, China;
3. The Analysis and Testing Center of Harbin Institute of Technology, Harbin 150001, China)
Chinafgms@hit.edu.cn

Abstract: 65Si2MnWA steel has high strength after conventional quenching and tempering, but it is found that the plasticity is relatively poor in practical use. Therefore, we hope to make use of the Q&P treatment to improve the strength and toughness of the material. Through OM, XRD, SEM, TEM, and electronic universal testing machine, the influence of two-step Q&P treatment on the microstructure and properties of 65Si2MnWA is systematically investigated.

Fig.1 shows the mechanical properties of 65Si2MnWA steel under different processes. It can be seen that the material has the best performance after being isothermally quenched at 180 ℃ and then partitioned at 330 ℃ for 20 min. Compared with the conventional process, the yield strength under this process is basically unchanged, but the tensile strength is slightly improved, from 1814 MPa to 1948 MPa, and especially the elongation rate is greatly increased, from 7.6% to 17.8%. Fig.2 shows the distribution of austenite and martensite in 65Si2MnWA steel under different processes. It can be seen from the figure that under the conventional quenching and tempering, the obtained austenite in the organization is very small and is calculated to be about 2.1%. However, through the two-step Q&P treatment, the content of austenite greatly increased to 18.2%. Fig.3 and Fig.4 show the grain size of the 65Si2MnWA steel under different heat treatment conditions. As can be seen from the figure, the microstructure processed by the conventional process and the Q&P process is very small, and the largest grain size is about 3 μm. Therefore, according to the Hall-Petch formula, the two treatments have higher strength, and are relatively close. However, the amount of austenite in the Q&P process is larger than that of the conventional process in both quantity and size, so the plasticity is much higher than that of the conventional process.

For 65Si2MnWA steel, the overall performance is best after quenching isothermally at 180 ℃ and then distributed at 330 ℃ for 20 min. Compared with the conventional process, the yield strength under the process remains basically unchanged, and the tensile strength slightly increases from 1814 MPa to 1948 MPa and the elongation rate significantly increases from 7.6% to 17.8%.

Quantitative characterization of the microstructure under different processes was performed by EBSD. It can be seen that the austenite content of the two-step Q&P process is much higher than that of the conventional process, so its plasticity is much higher than the plasticity of the conventional process. And the grain size of the two is comparable, so according to the Hall-Petch formula, their strength is basically the same.

Keywords: 65Si2MnWA steel, Q&P treatment, microstructure, mechanical properties

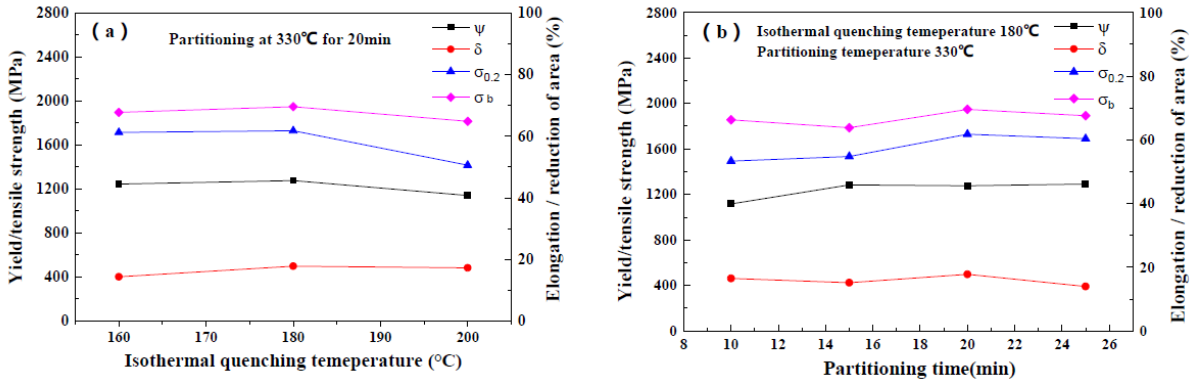

Fig.1 Test results of mechanical properties of 65Si2MnWA steel under different processes: (a) different isothermal quenching temperature; (b) different partitioning time

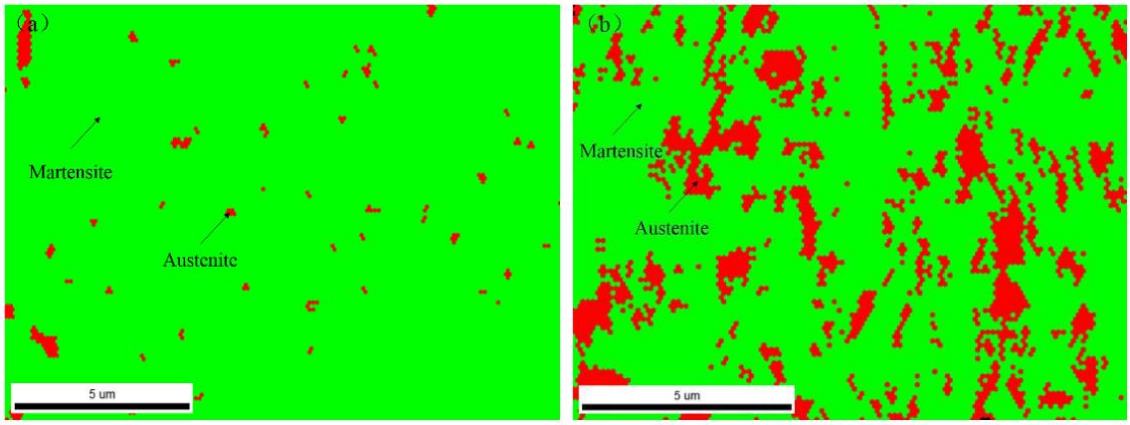

Fig.2 Austenite and martensite distributions characterized by EBSD: (a) conventional process; (b) Q&P process

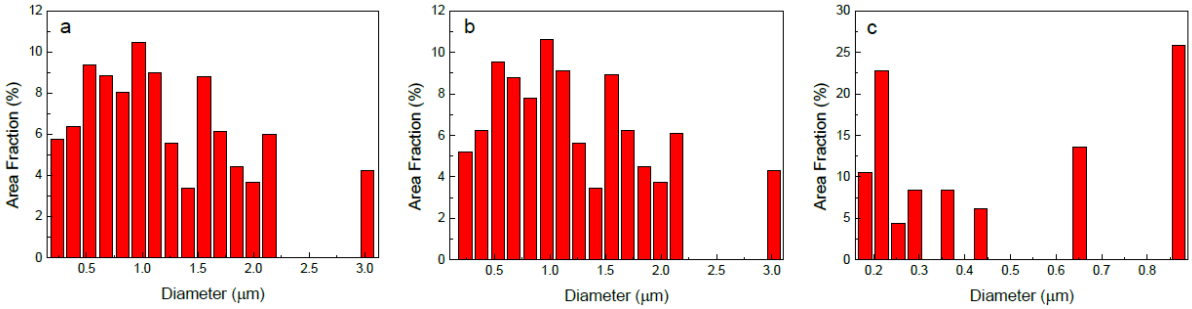

Fig.3 Grain size of conventional process: (a) overall grain size; (b) martensite grain size; (c) austenite grain size

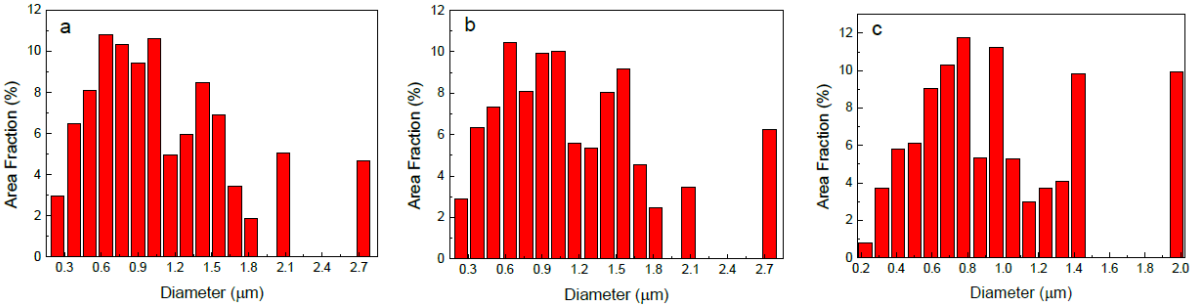

Fig.4 Grain size of Q&P process: (a) overall grain size; (b) martensite grain size; (c) austenite grain size

Microstructure of retained austenite and its strengthening toughening mechanism in 300M steel

Danni Yang, Hui Wang, Yong Liu, Zhonghong Lai, Jingchuan Zhu
(1. School of Materials Science and Engineering, Harbin Institute of Technology, Harbin 150001, China;
2. National Key Laboratory for Precision Hot Processing of Metals, Harbin Institute of Technology, China;
3. The Center of Analysis Measurement of, Harbin Institute of Technology, Harbin 150001, China)
ydn_cqu2012@163.com

Abstract: The commercial ultrahigh-strength low alloying steel 300M has been modified by adding the alloying elements of sicilion and vanadium in 4340 steel. 300M are widely used in aerospace, automobile manufacturing and other fields due to the high strength over 1500MPa, good fracture toughness and fatigue behavior. However, the common heat treatment limits a wider application of the steel because of poor toughness. Up to now, some practical method was put forward, such as quenching & tempering, Q&P and so on. In this work, a novel heat treatment method was proposed for improving the ductility without sacrificing ultra-high strength. The optimized isothermal quenched and tempered 300M reaches the δ_b of 16.8%, the $\sigma_{0.2}$ of 1669 MPa and the σ_b of 1738 MPa respectively. The bainite was obtained by using the novel heat treatment of isothermal quenching & tempering, meanwhile; the role of nano-scale retained austenite was researched in contribution to improve the mechanical properties of steel. The strengthening-toughening mechanism of retained austenite in 300M steel will be proposed.

The 300M steel used in this investigation was dual vacuum melted and was fully annealed. The composition of the steel is given in Table1. The specimen was austenitized at 900 ℃ in furnace, then quenched at 280 ℃ in the salt bath furnace for 3 h and tempered at 300 ℃ for 2 h. The volume fraction of the retained austenite of samples were analyzed by D/max-rB X-ray diffractometer (XRD) with Cu K radiation. The volume of the retained austenite was calculated according to GB8362-87. Scanning electron microscopy (SEM) was used for observing the microstructure of fracture. The morphology and distribution of retained austenite after heat treatment was observed by Electron back scattered diffraction (EBSD), and subsequently were analyzed by a transmission electron microscopy with selected area electron diffraction (SAED).

The novel heat treatment of isothermal quenching at 280 ℃ and tempering at 300 ℃ for 120 min can successfully enhance the mechanical properties of 300M steel, the δ_b, $\sigma_{0.2}$ and σ_b are 1738 MPa, 1669 MPa and 16.8% respectively.

Both retained austenite and ferrite lath are in nano-scale, the width of retained austenite is about 50 nm. These retained austenite uniformly distribute between ferrite lathes.

Evenly distribution of fine retained austenite can improve the strength and toughness of the steel. The phase of BCC and FCC accord with the orientation relationship of K-S. A volume of substructure and tangled dislocation during heat treatment can improve the strength of 300M steel as well.

Keywords: 300M steel, retained austenite, strengthening-toughening mechanism

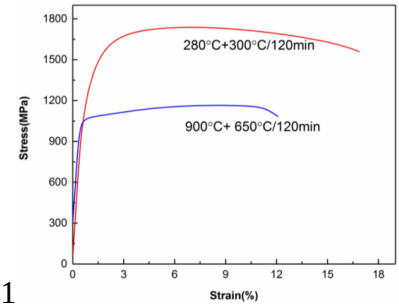

Fig.1

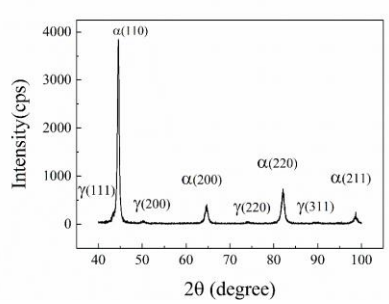

Fig.2

Fig.1 Engineering stress-strain curve of the alloys under different conditions

Fig.2 XRD patterns of the 300M steel after isothermal quenching and tempering heat treatment

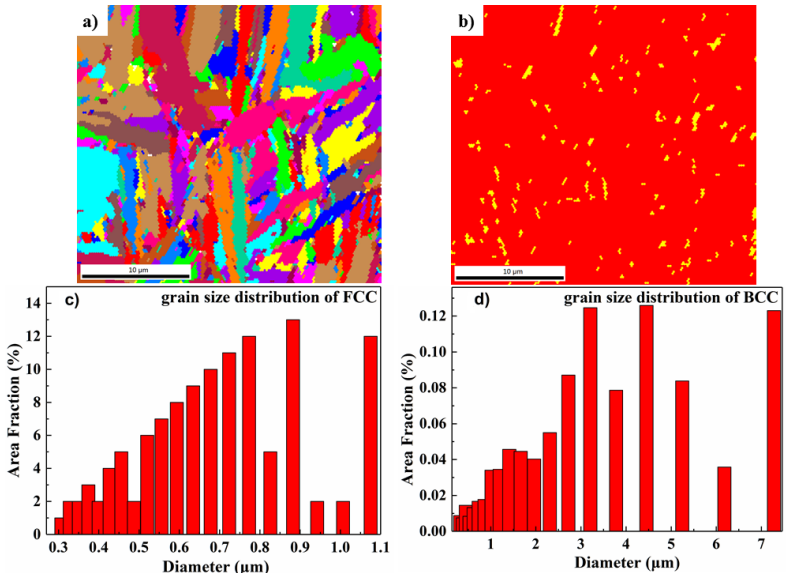

Fig.3 EBSD patterns of the 300M steel after isothermal quenching at 280 ℃ and tempering at 300 ℃ for 120 min: (a) orientation distribution; (b) phase distribution; (c) and (d) the distributions of austenite and bainite respectively

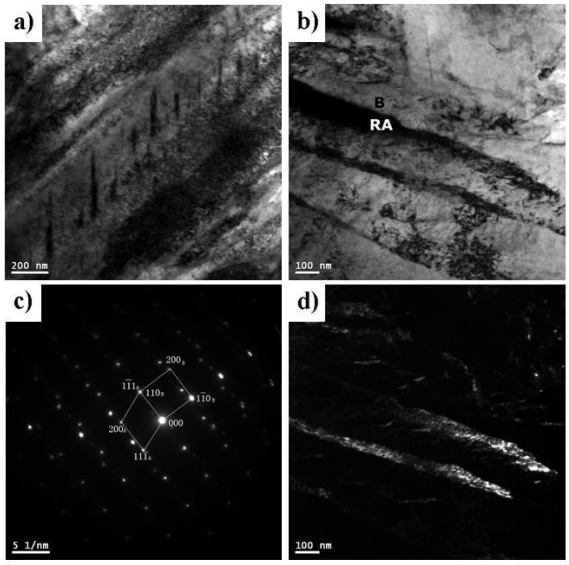

Fig.4 TEM image of the 300M steel after isothermal quenching at 280 ℃ and tempering at 300 ℃ for 120 min: (a) bright-field image of bainite; (b) ferrite lath; (c) SAED pattern of BCC phase along [001] zone axis and FCC phase along [011] zone axis; (d) dark-field image of retained austenite

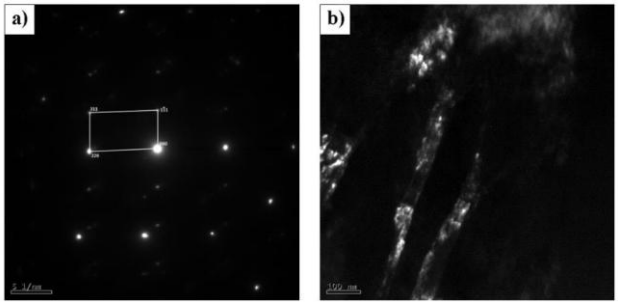

Fig.5 Transmission electron micrographs of retained austienite: (a) SAED pattern of retained; austinite along [$\bar{1}\bar{1}2$] zone axis; (b) dark-field image of retained austenite

Effect of dissociated NH_3 Gas at the several of filament temperatures in the gas nitriding

Sunkwang Kim, Jun-ho Kim
(KITECH)
jhkim81@kitech.re.kr

Abstract: In the present industry, gas nitriding is applied to improve the mechanical properties and corrosion resistance of structural steel or metal mold. However, a large of the gas nitriding process time is required to increase the thickness of the compound layer, which greatly affects the mechanical properties of the steel. To improve the growth rate of compound layer, in this study, we first dissociated NH_3 gas using the high temperature filament and gas nitriding was performed with the dissociated NH_3 which may be in NH or NH_2 states of a disconnection of one or two hydrogen atoms. The reason is that NH or NH_2 gases reaches the surface of the steel, the remaining one or two hydrogen atoms in the gases can easily be broken on the steel surface and nitrogen atom can easily be jumped and diffused into the steel.

To investigate the effect of dissociated NH_3 gas on the gas nitriding according to the filament temperature, it was changed of 0 ℃ and from 600 ℃ to 1600 ℃ with intervals of 200 ℃ at a pressure of 0.5 atm and the gas nitriding was performed for 6 hrs. Further experimental conditions are shown in Table 1, and in all the gas nitriding, the nitriding temperature was kept constant at 570 ℃.

Fig.1 shows cross-sectional photographs of the compound layer formed on the surface of pure iron when the gas nitriding was performed using dissociated NH_3 gas. The thickness of the compound layer continuously increases until the temperature reaches 1200 ℃, but the thickness of the compound layer rapidly decreases from above 1400 ℃, and it is the thinnest thickness at 1600 ℃. As shown in XRD result of Fig.2, the peak on γ'-Fe4N phase peaks were detected and the ε-Fe_{2-3}N phase peaks gradually decreased from 1400 ℃. The reason is that a large amount of the NH3 gas was decomposed from above 1400 ℃ and the nitriding potential value was decreased. To analyze the nitrogen concentration in the compound layer, the nitrogen concentration distribution along the depth was measured as shown in Fig.3. The surface nitrogen concentration was over 5.6wt% up to 1200 ℃, but the surface nitrogen concentration was below 5wt% from above 1400 ℃.

In the present study, it is possible to form a thick compound layer on the surface in a short time using the NH_3 gas dissociated in gas nitriding up to 1200 ℃. However, when NH_3 gas was almost decomposed above filament temperature of 1400 ℃, the nitriding potential was decreased because NH_3 gas was dissociated to stable states of N_2 and H_2 gas. As the results, the growth rate of compound layer was decreased. That is, when the gas nitriding is performed using the dissociated NH_3 gas, the growth rate of compound layer is increased.

Keywords: NH_3 dissociation, gas nitriding

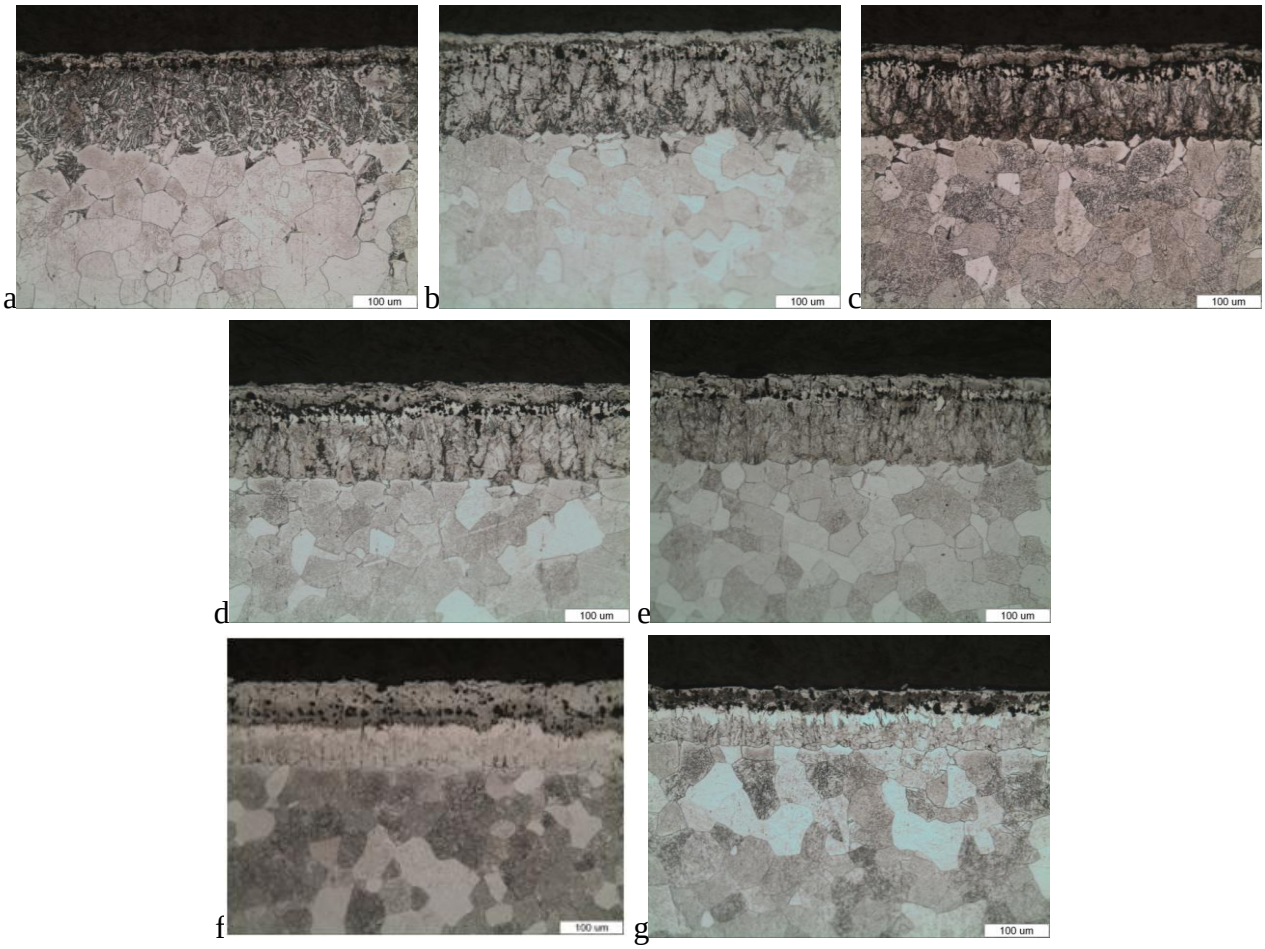

Fig.1 Optical micrographs near the surface in the cross section after the treatment of gas nitriding using dissociated NH_3 gas by the several of filament temperatures: (a) 0 ℃; (b) 600 ℃; (c) 800 ℃; (d) 1000 ℃; (e)1200 ℃; (f)1400 ℃; (g) 1600 ℃

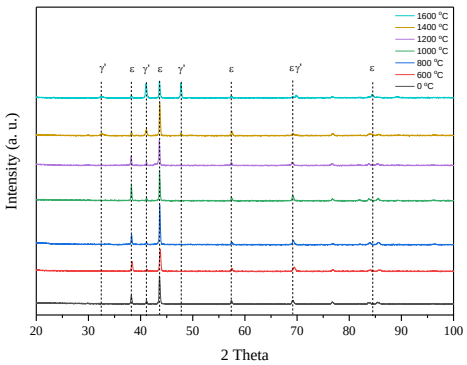

Fig.2

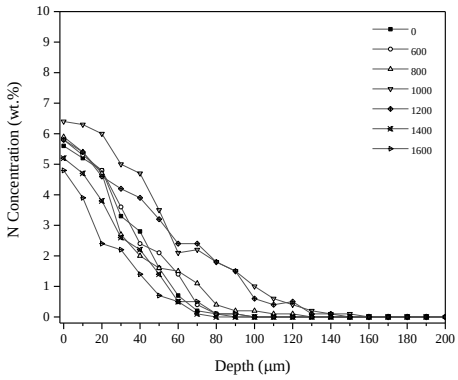

Fig.3

Fig.2 Diffraction spectra of the gas nitrided pure iron using dissociated NH_3 gas at the several of filament temperatures

Fig.3 Weight percentage of nitrogen vs depth from surface of the gas nitrided pure iron using dissociated NH_3 gas at the several of filament temperatures

Effect of annealing process on mechanical properties of tungsten-rhenium alloy wires

Xinwei Bo[1], Qi Liu[1], Yuchun Wang[2], Wenjing Hu[2], Yuanyuan Wu[2], Xiaoyu Wang[1], Chundong Jiang[1], Yanhui Wang[1], Haoran He[1], Chengchao Liu[1], Demao Chen[1]
(1. Chongqing Materials Research Institute Co., Ltd.;
2. Nanjing Sanle Eletronic Information Industry Group Co., Ltd.)
cqccy@qq.com

Abstract: The tungsten-rhenium alloy wires (WRe20) was prepared by powder metallurgy process, further, the change of mechanical properties with annealing temperature, annealing time, and other factors were studied for the wire which diameter is ϕ0.4 mm, ϕ0.104 mm or ϕ0.075 mm by the means of batch annealing and continuous annealing. The study found that it is difficult to obtain good mechanical properties of ϕ0.4 mm wire by the continuous annealing at different temperatures for 1m/s speed annealing, while we can obtain the best tensile strength and elongation for ϕ0.104 mm wire at the conditions of 1100 ℃ and 18 m/s speed; by the batch constant temperature annealing at 1350 ℃ for 45 mins, the wires whether ϕ0.104 mm or ϕ0.4 mm always have not split or broken when it be bent fold 180°. For the ϕ0.075 mm Tungsten-Rhenium alloy wire. The tensile strength of the wire was 2028 MPa, the elongation after breaking was 16% when annealed at 1300 ℃ for 30 min., but The tensile strength reduced to 1800 MPa and ductility rose to 18.6% when the wire was annealed at 1420 ℃×30 min. So, the tensile strength decreases significantly while the elongation significantly increases as the annealing temperature rises.

Keywords: tungsten - rhenium alloy wire, heat treatment, resistant to bending, tensile strength

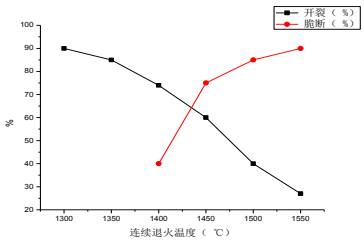

Fig.1 Effect of continuous annealing on bending fold of 0.4 mm wire

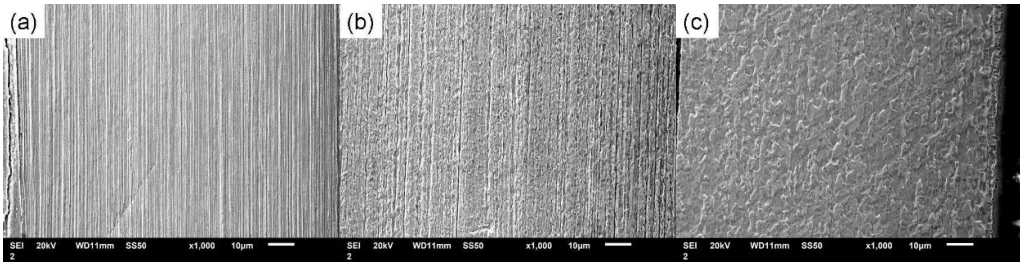

Fig.2 SEM images of samples in different heat treated process: (a) as-worked condition; (b) 1350 ℃ for 45 min; (c) 1450 ℃ for 45 min

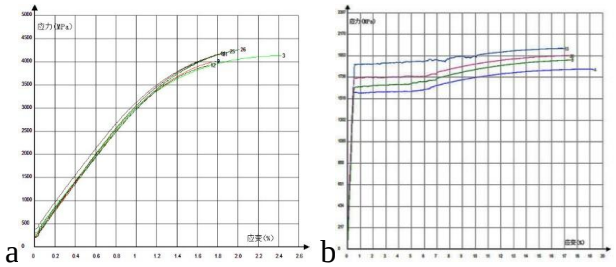

Fig.3 Tensile strength of 0.104 mm continuous annealing (a) and tensile strength of 0.075 mm isothermal annealing (b)

Effect of cold rolling on mechanical properties of Al-0.1Sc-0.05Zr alloy during solution aging

Heng Li, Zhiyong Luo, Zhen Wang, Yue Hu, Wenchao Shi
(Hefei University of Technology)
liheng0205@hfut.edu.cn, shiwenchaohfut@hfut.edu.cn

Abstract: Because of its high strength and toughness, Al-Sc-Zr alloy is widely used in aerospace, high-speed trains and welded load-bearing structural parts of ships and other fields. Therefore, the research of Al-Sc-Zr alloy has become one of the hotspots in recent years. In this paper, the Al-0.1Sc-0.05Zr alloy is treated with 300 ℃ 465min after solution at 600 ℃. The effect of different cold rolling deformation on the solution aging of Al-0.1Sc-0.05Zr alloy was investigated by means of 465min treatment.

The hardness, microstructure and tensile properties of Al-0.1Sc-0.05Zr alloys in different states were analyzed by using HV-5 type low load Wechsler hardness tester (AXIO) Lab.A1 metallographic microscope SU8020 scanning electron microscope and CMT-5105 microcomputer controlled electronic universal testing machine. It was found that the time of reaching the peak value was 465 min after the peak aging of 600 ℃ solution at 300 ℃, and the hardness, tensile strength and yield strength of the alloy were obtained after the peak aging. The hardness, tensile strength, yield strength and elongation of the alloy treated with #number0# ℃ solution 40% cold deformation at 300 ℃ were 57.25 HV, 147 MPa, 1123.6 MPa, and 12.29%. The hardness, tensile strength and tensile strength of the alloy treated with 465 min after 60% cold deformation at 600 ℃ were treated with 60% solution at 600 ℃.The hardness, tensile strength, yield strength and elongation of the alloy treated with 80% cold deformation at 600 ℃ after aging at 300 ℃ are 60.16 HV, 212 MPa, 38.3 MPa, and 8.33%. the yield strength and elongation of the alloy are 59.26 HV, 169 MPa, 125.7 MPa, and 11.187%. The hardness, tensile strength, yield strength and elongation of the alloy treated with 80% cold deformation at 600 ℃ are 60.16 HV, 212MPa, 138.3 MPa, and 8.33%, respectively.

After comparison, it was found that after aging at 600 ℃ solution at 300 ℃, the dislocation density in the microstructure of Al-0.1Sc-0.05Zr alloy was small and the content of strengthening phase precipitated in aging process was less, while the mechanical properties of 465 min treated with 80% cold deformation at 600 ℃ were the best after aging treatment at 300 ℃. This is because the dislocation density in the microstructure increases after cold rolling, and the larger the deformation amount, the greater the dislocation density in the microstructure, and the precipitation and dispersion of the Al_3(Sc, Zr) strengthening phase with core-shell structure in the microstructure after aging at 300 ℃ at high temperature. It can effectively block the slip of dislocation and the migration of subgrain boundary. The whole process mainly utilizes the interaction of hardening and aging strengthening methods. The results can provide theoretical support and technical basis for the wide application of Al-0.1Sc-0.05Zr alloys.

Keywords: Al-0.1Sc-0.05Zr alloy, cold rolling, thermomechanical treatment, mechanical properties

Changes of microstructure and mechanical properties of 6061 aluminum alloy by friction stir processing under different heat treatment conditions

Ming Li, Heng Li, Zhiyong Luo, Yuan Si, Yucheng Wu
(Hefei University of Technology)
liheng0205@hfut.edu.cn, ycwu@hfut.edu.cn

Abstract: Friction stir processing is a new kind of modification method for large plastic deformation of materials. In this paper, the effects of friction stir on the macroscopic morphology, microstructure, hardness and tensile strength of 6061 aluminum alloys after solid solution and aging were studied. The results show that, after friction stirring, there are obvious hole defects in the bottom of the stirring zone of the 6061 aluminum alloy with solid solution, while the microstructure of the stirring zone of the aging 6061 aluminum alloy is complete. The cross section structure of 6061 aluminum alloy in two heat treatment states are similar, and the whole stirring zone has fine equiaxed recrystallized grains. The heat affected zone has obvious interface with the stirring zone in the forward side, but interface in the backward side is not obvious and has a gradual trend. The fine dynamic recrystal grains can be found between the two sides of the heat affected zone, and it is also found that the range of the interface between the stirring zone and the forward side is different in the two heat treatments. The interface of the alloy with solid solution changes slowly, but the alloy with aging is steeper. The hardness experiments of 6061 aluminum alloy were carried out respectively in the direction perpendicular to the direction of friction stir processing after two kinds of heat treatments and the rules are generally consistent. The hardness of the processing zone is obviously lower than that of the base metal area, and with the increase of the distance from the machining center, the hardness gradually recovers to the base metal hardness. The results show that the distribution of microhardness perpendicular to the thickness direction of the aged 6061 aluminum alloy are W shape both in friction stir processing and in the direction perpendicular to the plate thickness after aging. The distribution of microhardness perpendicular to the thickness of solid solution 6061 aluminum alloy is U-shaped in general after friction stir processing and aging. The distribution of hardness in the forward side and the backward side are not completely symmetrical in the two states both after friction stir processing and aging. The hardness of the stirring zone of the two kinds of heat-treated alloys are lower than that of the base metal. The hardness of the 6061 aluminum alloy in two states are distributed in N shape in the direction of plate thickness after friction stir processing and aging. The hardness of the upper part of the stirring zone is the highest, and the tensile strength and elongation of the two states of 6061 aluminum alloy after friction stir processing and aging have little difference. In addition, the hardness, elongation and tensile strength of friction stir zone in aging 6061 aluminum alloy after friction stir processing are 74 HV, 346 MPa and 24.7% respectively. Then the 6061 aluminum alloy was heat preserved at 180 ℃ for 6 hours and the hardness, elongation and tensile strength of stirring zone are 107 HV, 397 MPa and 13.2% respectively. The results can provide theoretical basis and technological support for friction stir processing of aluminum alloy.

Keywords: 6061 aluminum alloy, microstructure, friction stir processing, aging, solution

Latest developments of deep cryogenic treatment

Kaikai Wang[1], Kaixuan Gu[1], Zeju Weng[1], Jianpeng Zheng[2], Junjie Wang[1]
(1. Technical Institute of Physics and Chemistry, Chinese Academy of Sciences (CAS);
2. Department of Mechanical and Electrical Engineering, Xiamen University)
wangjunjie@mail.ipc.ac.cn

Abstract: For further improving the performance of materials, deep cryogenic treatment (DCT) has been developed as a complementary process of traditional heat treatment for many decades. As an effective modification method, it can improve the wear resistance, dimensional stability and comprehensive mechanical properties of different materials (such as steels, aluminum alloy, titanium alloy and so on). Compared with conventional heat treatment, the effect of DCT on mechanical properties is not so obvious. But the DCT can always improve the service life of materials dramatically and DCT has been applied in aerospace industry, advanced manufacturing industry and sophisticated instruments by our team. The effect of DCT processes on several typical materials following strengthening mechanism and the microstructure evolution are presented briefly in this paper. Furthermore, the applications in different fields of DCT, latest research progress and prospects are introduced.

The effect of DCT on a bainitic steels with bainite/martensite (B/M) multiphase microstructure was studied to elucidate the positive effect of DCT on structure and mechanical properties. The study indicates that DCT can improve mechanical properties and wear resistance of bainitic steels. It reduces the content of blocky martensite/austenite (M/A) constituents by eliminating unstable retained austenite (RA). At the same time, RA is relatively more enriched in carbon after DCT, compared to the tempering process. During DCT, the brittle martensite is also avoided, since the enhanced recovery reduces the carbon concentration during tempering. DCT effectively improves the mechanical properties (including strength, elongation, toughness and hardness). A good combination of strength and ductility are obtained after deep cryogenic treatment and tempering at 280 ℃ (ultimate tensile strength: 1389 MPa; total elongation: 17.1%; U-notch impact toughness at 20 ℃: 78 J/cm^2). DCT reduces the blocky M/A constituents by eliminating unstable RA, and improves the stability of RA with higher carbon-contents. The supersaturation of martensite in carbon-content is relieved on tempering after cryogenic treatment, which benefits the mechanical properties to avoid brittleness. The recovery of martensite leads to precipitation of carbides and contributes to hardness and wear resistance.

DCT has been an effective method for modification of materials. It is usually combined with the traditional heat treatment of steels. However, the effect of its combination with the heat treatment of metastable β titanium alloy still remain unknown. Microstructure evolution in TB8 metastable β titanium alloy subjected to DCT was investigated experimentally. DCT was conducted on annealed TB8 alloy (RC) directly, prior to aging treatment (SCA) and after aging treatment (SAC), respectively. Tensile properties and microhardness were tested to evaluate the effect of DCT on mechanical properties. The results showed that RC and SAC both have no influence on the tensile properties and microhardness of TB8 alloy, while strengthening effects were obtained by SCA compared to the conventional solution and aging treatment (SA). Refinement and homogenization of α precipitates were induced by the additive of DCT.

Deep cryogenic treatment can also significantly improve the wear resistance and cutting performance of cemented carbide, effectively extend the service life of cemented carbide tools, but have little effect on the hardness and toughness.

Keywords: cryogenic treatment, microstructure, hardness, wear resistance, residual stress

Study on plasma spraying process and corrosion resistance of NdFeB alloy surface

Cheng Gao
(Guilin University of Electronic Technology)
116710709@qq.com

Abstract: NdFeB permanent magnet alloys have excellent magnetic properties and mechanical processing characteristics, but because of their rich yttrium elements, the chemical properties are lively, and NdFeB permanent magnet alloys are generally prepared by the sintering process, and there are a lot of micropores on the surface. The micro-structure is loose. This makes the neodymium-iron-boron permanent magnet extremely corrosive due to the galvanic effect in a hot and humid environment. Plasma spraying technology was used to protect the surface of NdFeB permanent magnet alloy and Al_2O_3 ceramic layer was prepared to improve its corrosion resistance. In this study, the spraying voltage, the spraying current, the main gas flow rate and the spraying distance in the plasma spraying process were selected as the factor variables of the process parameters, and the orthogonal test optimization was performed. The test includes the determination and analysis of the average micro-hardness of the ceramic layer of the sample, the determination and analysis of the bonding strength of the ceramic layer, the assessment of the macroscopic appearance of the salt spray corrosion of the ceramic layer, and the determination and analysis of the corrosion rate of the ceramic layer in 3.5wt% NaCl solution. The results show that the average micro-hardness of the ceramic layer exceeds 790 HV0.3 and the highest can reach 900 HV0.3. The sample was continuously sprayed with (3.5±0.2)wt% NaCl solution, and the macroscopic morphology of the ceramic layer after 250 h was graded according to the percentage of surface defects, and the best ceramic layer quality was 0 grade, indicating that the coating has excellent The corrosion resistance. The best set of samples had a corrosion potential of -380 mV and a corrosion current of 0.0010 mA cm^{-2}. The single phase of γ-Al_2O_3 contained in the ceramic layer reacts with H^+ and $(OH)^-$ to form free Al^{3+} and $(AlO_2)^-$. The reason for the different rate of corrosion weight loss is that Al_2O_3 and (OH)react to $Al(OH)_3$. Colloids, in turn, continue to react to form free $(AlO_2)^-$ ions, which have a deterrent effect on the rate of corrosion weight loss. Orthogonal experiments show that the primary and secondary influence law of the process factors on the corrosion resistance of the ceramic layer is spray voltage > spray distance > main gas flow > spray current, and the intensity ratio is about 4:1.25:1:1, which is in the range of selected factors. The optimal coating process parameters for the corrosion resistance of the inner ceramic layer were a spraying voltage of 48 V, a spraying current of 450 A, a main gas flow of 2300 L/h, and a spraying distance of 115 mm.

Keywords: plasma spraying technology, ceramic layer, corrosion resistance

Formation of coherent microstructure with cuboidal nanoprecipitates in BCC-based high-entropy superalloys and their microstructural stability

Qing Wang, Chuang Dong
(Dalian University of Technology)
wangq@dlut.edu.cn

Abstract: The particle morphologies of ordered phases (B2 and L21) in body-centered-cubic (BCC) matrix is closely related to the lattice misfit between B2/L21 and BCC, in which the lattice misfit depends mainly on the chemical compositions of these two phases. The multiprincipal component alloying of high-entropy alloys (HEAs) will provide a new composition pathway for adjusting the lattice misfit between BCC and B2/L21. The present work designed a series Al-Ti-Ni-Co-Fe-Cr alloys with compositions of [(Al/Ti)-TM14](Al/Ti) in light of the cluster formula approach to investigate the relationship between coherent morphologies (weave-like spinodal microstructure, spherical precipitation, and cuboidal precipitation) and the lattice misfit. Among them, the microstructure of cuboidal B2/L21 nanoprecipitation into the BCC matrix renders the HEAs with not only high strength but also good ductility, similar to those in Ni-base superalloys, i.e., cuboidal L12 nanoparticles embedded in FCC matrix. Then, the relationship between coherent microstructure and lattice misfit was extended to several BCC-based alloy systems containing ordered phase precipitation to verify its validity. In addition, the optimal strengthening as a function of the size of the coherent precipitates is discussed via the precipitation strengthening mechanism. The present work also addressed the microstructural stability (i.e., the microstructural evolution with temperature) of HEAs. Especially, the B2 nanoprecipitates in BCC-based Al-Ni-Co-FeCr system were not coarsened after long-term aging at 500-600 ℃ for 1068 h, indicating that the B2 nanoprecipitates have a high stability below this temperature.

Keywords: high-entropy superalloys, coherent microstructure, particle shape, microstructural stability, precipitation strengthening mechanism

Grain refinement and mechanical properties of a Fe-30Mn-0.11C steel

JianMei Kang, Yuhui Wang
(Yanshan University)
yhwang@ysu.edu.cn

Abstract: A fully recrystallized ultrafine-grained (UFG) Fe-30Mn-0.11C steel with a mean grain size of 1 μm was successfully produced using conventional cold rolling and annealing process.
The UFG Fe-30Mn-0.11C steel exhibited a high tensile ductility (~60.4%) and yield stress (381 MPa). Grain refinement and dislocation source hardening were responsible for showing such combination of strength and ductility of the studied material.

Keywords: fully recrystallization, ultrafine-grain, grain refinement, source hardening

Studies on attractive MoAlB ceramics: hot pressing sintering process and its high temperature oxidation resistance

Yichao Gong, Wenbo Ye, Guojun Zhang
(School of Materials Science and Engineering, Xi'an University of Technology)
zhangguojun@xaut.edu.cn

Abstract: Molybdenum aluminum boride (MoAlB) is a ternary transition metal boride, which has promising aeronautic and high-temperature applications due to its excellent mechanical property, favorable thermal conductivity and fantastic high temperature oxidation resistance etc. In this work, Mo-Al-B powders with different molar ratio were prepared by mechanical alloying process to obtain fine particles and narrow distribution, and then vacuum hot-pressing sintering (39 MPa) was employed to obtain the MoAlB ceramics at 1300 ℃ for 2.5 h. XRD analyses showed that the samples had high phase purity when the molar ratio of Mo, Al and B was 1:1.3:1. Furthermore, the hardness, bending strength, fracture toughness and compressive strength of MoAlB were tested, the results showed that the sample with fine grain and high content of MoAlB phase possessed optimum comprehensive mechanical performances, and the fractures model of the MoAlB during the tests of bending were the mix of transgranular and intergranular. The oxidation behavers of MoAlB in air was studied in the 1000-1300 ℃ temperature range for 30 h, the results suggested the prepared MoAlB ceramics had favorable high temperature oxidation resistance, and the related mechanism was also discussed. The surface of MoAlB is rapidly oxidized to form oxide scales, and then with the volatilization of B_2O_3 and MoO_3, Al_2O_3 layer gets dense and covers on the surface of MoAlB substrate. Finally, the Al_2O_3 coating will protect MoAlB from the further corrosion.

Keywords: MoAlB, hot pressing sintering, high temperature oxidation resistance

Development of walking beam furnace for forging heating aluminum alloy billet of wheel hub

Wenliang Zhang, Ping Luo, Hang Su, Tong Zhou
(Beijing Research Institute of Mechanical and Electrical Technology, Beijing, 100083, China)
zhangwlwork@163.com

Abstract: Introduced the develop process of walking beam furnace for the aluminum alloy billet heating before forging, which used to make the wheel hub of bus or truck. Production practice proven that this furnace is in such advantages as high heating speed, high production, high temperature uniformity between core and surface, low energy consumption, high level of automation and running stabilization. The billet as heating with the furnace can meet the requirement of the temperature and can provide a good foundation for next forging.

Keywords: aluminum alloy wheel hub, forging heating, walking beam furnace, temperature uniformity

Heat treatment effects on the microstructure and mechanical properties of 11Cr-3Co-2.3W martensitic heat resistant steel

Chenshuo Cui[1], Xiuhua Gao[1], Guanqiao Su[1], Cairu Gao[1], Zhenguang Liu[2], Chenglin Zhu[3]
(1. Northeastern University; 2. Jiangsu University of Science and Technology;
3. China Power Complete Equipment Co., Ltd.)
xiuhuagaoneu@126.com

Abstract: Effects of normalizing and tempering heat treatment on microstructure and properties of 11Cr-3Co-2.3W martensitic heat resistant steel were studied by the optical microscope, XRD, SEM and TEM. The results reveal that the best combination of excellent impact and tensile properties can be achieved by normalizing at 1050 ℃ for 0.5 h and tempering at 780 ℃ for 2 h. The combinations in the present steel are: Charpy impact energy: 104 J, YS: 716 MPa, UTS: 898 MPa and elongation: 22.4%. $M_{23}C_6$ carbide particles are almost dissolved when the temperature is elevated to 1150 ℃. The austenite grain coarsens obviously with elevating normalizing temperature from 1050 ℃ to 1150 ℃. Since the new austenite formed at high tempering temperature of 850 ℃ transforms into martensite during the following annealing process, both the yield strength and UTS increase, whereas its impact properties decrease.
Keywords: mechanical property, heat treatment, strength, precipitation, martensite

The process optimization of organic-inorganic hybrid perovskite thin film

Tianyi Han, Yong Liu, Jingchuan Zhu, Zhonghong Lai
(Harbin Institute of Technology)
lyonghit@hit.edu.cn, fgms@hit.edu.cn

Abstract: Organic-inorganic hybrid perovskite solar cells have developed rapidly due to its low temperature fabricating, high stability and low cost, just a few years since it was found in 2009. Its photoelectric conversion efficiency (PCE) has reached 22.1% from the original 3.8% to recently. As the absorbing material of solar cells, morphology of organic-inorganic hybrid perovskite thin film does great influence on photoelectric conversion efficiency of solar cell. In this paper, we report a solution-based hot-casting technique to achieve a uniform perovskite thin film with good photoelectric properties.
Keywords: process optimization, organic-inorganic hybrid perovskite, thin film

Effect of heat treatment process on ZrW_2O_8 synthesis by hydrothermal method

Longzhi Zhao
(School of Materials Science and Engineering)
454106741@qq.com

Abstract: The negative thermal expansion ZrW_2O_8 material was prepared by hydrothermal method. The mechanism of hydrothermal reaction and the morphology and purity of the synthesized products were studied. The results showed that Zr^{4+} formed a Zr^{4+} four polymer in the process of adding zirconium chloride in the process of adding, and the gel phenomenon was produced in the experiment. The shape of the synthetic product ZrW_2O_8 is a regular bar with a purity of 99.54%.
Keywords: hydrothermal method, negative thermal expansion